

1
2 **Author Response to Interactive Comment by Anonymous Referee #1 on**
3 **“ORCHIDEE MICT-LEAK(r5459), a global model for the production, transport and**
4 **transformation of dissolved organic carbon from Arctic permafrost regions, Part**
5 **1: Rationale, model description and simulation protocol” by Simon P. K. Bowring**
6 **et al.**

7
8 Dear Anonymous Referee #1,

9
10 Thank you for taking the time to read and review our manuscript, and in doing so
11 providing such diligent and constructive commentary for its improvement, which we
12 hope we have been able to assimilate into its content to the greatest degree possible in
13 our responses, which follow below.

14
15 **Specific Comments**

16
17 **Line 46: the “migration of permafrost line” really only makes sense on a map.**
18 **Perhaps rephrase.**

19 Thank you for spotting this conceptually misleading description in our text. The phrase
20 has now been modified to
21 *“... as the boundary between discontinuous and continuous permafrost migrates poleward*
22 *and toward the continental interior over time.”*

23
24 **line 50: the authors pulled out some very high number, I don't know where this**
25 **came from. McGuire 2009 estimates a lateral flux of 80 Tg C and a net “arctic” land**
26 **sink of 600-800 Tg C. That makes the DOC component ~10% of NEP.**

27
28 Again, thank you for spotting this, which indeed looks misleading, and comes from
29 taking a mix of upper and lower bounds for lateral flux and NEP, respectively. However,
30 we can't find the 600-800TgC /yr sink you refer to in the reference cited. Referring to
31 McGuire et al (2009) Table 2, the inversion-based terrestrial sink from Rödenbeck et al
32 (2003) is 400 TgC/yr, that from Baker et al (2006) is 190 TgC/yr, and that from Gurney
33 et al. (2003) is 230 TgC/yr. Because these estimates exclude the European Arctic,
34 McGuire estimates that the 'true amount is 'less than' 0.5 PgC/yr which, given the
35 uncertainty range from the inversion studies, means that he accepts the range of the net
36 CO₂ sink as being 0-800TgC yr. In Table 6 of McGuire et al., indeed the lateral carbon
37 flux is 39 TgC/yr excluding DIC and 83 TgC/yr with it.

38
39 In our manuscript text body, we write that “ the yearly lateral flux of carbon from soils
40 to running waters may amount to ~40% of net ecosystem carbon exchange”. This
41 implies the total lateral carbon flux, and not the DOC. Thus, from a mid-point of 400
42 TgC/yr from the above-mentioned 0-800TgC/yr, we re-write the sentence as follows:

43
44 *“[...] the yearly lateral flux of carbon from soils to running waters may amount to about a*
45 *fifth of net ecosystem carbon exchange (~400 TgC yr⁻¹), about ~40% of which may be*
46 *contributed by DOC (McGuire et al., 2009). Excluding the dissolved inorganic carbon*
47 *component of this flux, as well as dissolved CO₂ input from soils, the vast majority (85%) of*
48 *riverine organic carbon discharge to the Arctic Ocean occurs as dissolved organic carbon*
49 *(DOC), as described in (e.g.) Suzuki et al. (2006).”*

50
51
52
53
54
55
56
57
58
59
60
61
62
63
64
65
66
67
68
69
70
71
72
73
74
75
76
77
78
79
80
81
82
83
84
85
86
87
88
89
90
91
92
93
94
95
96
97
98

155-156: I think these numbers need to be double checked. The point of this paragraph could be clearer.

The numbers have been double-checked and are as reported in McGuire et al. (2009), but now distinguish between total evasion and the water bodies from which these occur as follows:

" CO₂ evasion rates from Arctic inland waters (Fig. 1j,e,m), which include both lakes and rivers, are estimated to be 40-84 TgC.yr⁻¹ (McGuire et al., 2009), of which 15-30 TgC.yr⁻¹ or one-third of the total inland evasion flux, is thought to come from rivers. However, a recent geo-statistically determined estimate of boreal lake annual emissions alone now stands at 74-347 TgC.yr⁻¹ (Hastie et al., 2018), potentially lowering the riverine fraction of total CO₂ evasion. These numbers should be compared with estimates of Pan Arctic DOC discharge from rivers of 25-36 TgC.yr⁻¹ (Holmes et al., 2012; Raymond et al., 2007)."

AO: This is my preference, but it wouldn't add much space to write out Arctic Ocean and it would be more intuitive to follow.

This is an understandable preference, given the already large number of acronyms contained in the document. The text has been modified accordingly.

249-254: This paragraph is confusing. The points could be expanded and clarified

Indeed, we find the same. The paragraph has been shortened and merged with the preceding paragraph. The processes that are novel are described then later in the text.

"However numerous improvements in code performance and process additions post-dating these publications have been included in this code. Furthermore, novel processes included in neither of these two core models are added to MICT-L, such as the diffusion of DOC through the soil column to represent its turbation and preferential stabilisation at depth in the soil, as described in Section 2.11."

265-274: This is quite confusing and makes what is new here unclear.

We have now removed the first half of this paragraph and merged the remainder with the preceding, so as to avoid unnecessary complexity and confusion. The section removed is:

" Where these differences were so large as to prove a burden in excess of the scope of this first model version, such as the inclusion of the soil carbon spinup module, they were omitted from this first revision of MICT-L. The direction of the merge -which model was the base which incorporated code from the other -was from ORCHILEAK into MICT, given that the latter contains the bulk of the fundamental (high latitude) processes necessary for this merge."

289: This is the first mention of this site specifically, and it really comes out of nowhere. Consider introducing the site before this.

99
100
101
102
103
104
105
106
107
108
109
110
111
112
113
114
115
116
117
118
119
120
121
122
123
124
125
126
127
128
129
130
131
132
133
134
135
136
137
138
139
140
141
142
143
144
145
146
147

We agree with this observation, and have added in the following sentence at the end of the Introduction (line 264-267).

"The choice of the Lena River basin in Eastern Siberia as the watershed of study for model evaluation owes itself to its size, the presence of floodplains and mountain areas which allow us to test the model behavior for contrasting topography, the relatively low impact of damming on the river, given that ORCHIDEE only simulates undammed fluvial 'natural flow', and its mixture of continuous and discontinuous permafrost with tundra grassland in the north and boreal forests in the south, and is described in greater detail in Part 2 of this study"

430: Typo 437: typo

Extra full-stop removed.

444-446: Confusing. This sounds like a lake or pond

The section you refer to is: "Further, in modelled frozen soils, a sharp decline in hydraulic conductivity is imposed by the physical barrier of ice filling the soil pores, which retards the flow of water to depth in the soil, imposing a cap on drainage and thus potentially increasing runoff of water laterally, across the soil surface (Gouttevin et al., 2012). In doing so, frozen soil layers overlain by liquid soil moisture will experience enhanced residence times of water in the carbon-rich upper soil layers, potentially enriching their DOC load."

This refers to the frozen vertical barrier imposed by soil freezing on hydrological transfer to deeper layers. This is why they are referred to as 'liquid soil moisture' as opposed to water body or some such, as it implies that water increases its residence time in a certain layer above the frozen portion, but does not remain static there nor 'pond' into a water body proper.

We have also added the clarification that frozen water in the form of thick ice wedges that are important for e.g. thermokarst formation, are not simulated by the present model formulation, e.g. " Note that ice wedges, an important component of permafrost landscapes and their thaw processes, are not included in the current terrestrial representation, but have been previously simulated in other models (Lee et al., 2014)".

In addition, we found some potentially misleading text in the following segment: "First, in the process of drainage DOC is able to percolate from one layer to another, through the entirety of the soil column, meaning that vertical transport is not solely determined by 11th layer concentrations, given that DOC can be continuously leached and transported over the whole soil column. "

We have adapted this section as follows:

" First, as it water percolates through the soil column, it carries DOC along from one layer to another through the entirety of the soil column, but this percolation is blocked when the soil is entirely frozen, i.e. it is assumed that all soil pores are filled with ice which blocks

148 percolation. This implies that DOC transport is not just determined by what enters from the
149 top but also by the below ground production from litter, the sorption and de-sorption to
150 and from particulate soil organic carbon in the soil column, , its decomposition within the
151 soil column, and water vertical transport entraining DOC between the non-frozen soil
152 layers using the hydraulic conductivity calculated by the model as a function of soil texture,
153 soil carbon and time-dependent soil moisture (Guimberteau et al., 2018). "

154

155 **474: typo**

156

157 This has been corrected.

158

159 **4780480: confusing**

160

161 This refers to the following section of the manuscript: "The water residence time in each
162 reservoir depends on the nature of the reservoir (increasing residence time in the order
163 : stream < fast < slow reservoir). More generally, residence time decreases with the
164 steepness of topography, given by the product of a local topographic index and a
165 constant with decreasing values for the 'slow', 'fast' and 'stream' reservoirs."

166

167 To clarify this, we have shortened and increased the conciseness of the segment as
168 follows:

169

170 "More generally, residence time locally decreases with topographic slope and the grid-cell
171 length, used as a proxy for the main tributary length (Ducharne et al., 2003; Guimberteau
172 et al., 2012). This is done to reproduce the hydrological effects of geomorphological and
173 topographic factors in Manning's equation (Manning, 1891) and determines the time that
174 water and DOC remain in soils prior to entering the river network or groundwater."

175

176 In addition, to increase the readability of the subsection, descriptions of the hydrological
177 module in the paragraph preceding the segment you refer to are improved upon. The
178 original section reads: "The 'slow' water reservoir aggregates the soil drainage, i.e. the
179 vertical outflow from the 11th layer (2 m depth) of the soil column, effectively
180 representing 'shallow groundwater' storage. The 'fast' water reservoir aggregates
181 surface runoff simulated in the model, effectively representing overland hydrologic flow.
182 The 'slow' and 'fast' water reservoirs feed a delayed outflow to the 'stream' reservoir' of
183 the adjacent subgrid-unit in the downstream direction."

184

185 The model's hydrology routing scheme is indeed a complex system, and we use the same
186 terminology as that adopted by its architects cited to in the text, which in turn follow the
187 terminology given to these water reservoirs in the model code.

188

189 Thus we only try to make clearer the last sentence of the paragraph with the following
190 edit: " The 'slow' water reservoir aggregates the soil drainage, i.e. the vertical outflow from
191 the 11th layer (2 m depth) of the soil column, effectively representing 'shallow
192 groundwater' transport and storage. The 'fast' water reservoir aggregates surface runoff
193 simulated in the model, effectively representing overland hydrologic flow. The 'slow' and
194 'fast' water reservoirs feed a delayed outflow to the 'stream' reservoir' of the next
195 downstream sub-grid quadrant. "

196

197
198
199
200
201
202
203
204
205
206
207
208
209
210
211
212
213
214
215
216
217
218
219
220
221
222
223
224
225
226
227
228
229
230
231
232
233
234
235
236
237
238
239
240
241
242
243
244
245

498-490: Justification for this approach would be helpful (add supporting references)

We assume this refers to lines 498-500 and not 498-490. This segment reads:

"Active DOC flows into a Labile DOC hydrological export pool, while the Slow and Passive DOC pools flow into a Refractory DOC hydrological pool (Fig. 2b)."

This formulation follows on from prior published developments made to the model code, but is unpacked more explicitly in the section by adding the following content:

"However, because the terrestrial Slow and Passive DOC pools (Camino-Serrano et al., 2018) are given the same residence time, these two pools are merged when exported (Lauerwald et al., 2017): Active DOC flows into a Labile DOC hydrological export pool, while the Slow and Passive DOC pools flow into a Refractory DOC hydrological pool (Fig. 2b), owing to the fact that the residence time of these latter soil DOC pools is the same in their original (ORCHIDEE-SOM) formulation (Camino-Serrano et al., 2018), and retained and merged into a single hydrological DOC pool in Lauerwald et al. (2017). The water residence times in each reservoir of each subgrid-scale quadrant determine the decomposition of DOC into CO₂ within water reservoirs, before non-decomposed DOC is passed on to the next reservoir in the downstream subgrid quadrant."

In addition, to improve contextual understanding, in Section 2.3 (paragraph 1) we have added the following (in red) to this section: "The non-respired half of the litter feeds into 'Active', 'Slow' and 'Passive' free DOC pools, which correspond to DOC reactivity classes in the soil column in an analogous extension to the standard CENTURY formulation (Parton et al., 1987)."

508-525: These water pool names are really confusing.

527-534: I'm having a difficult time following this

Here we combine your two above comments into an adaptation to the paragraph as follows. We believe the confusion arises from our description of the fast, slow and stream reservoirs with respect to headwaters. The paragraph has been adapted as follows:

"Note that while we do not explicitly simulate headwaters as they exist in a geographically determinant way in the real world, we do simulate what happens to the water before it flows into a water body large enough to be represented in the routing scheme by the water pool called 'stream', representing a real-world river upwards of roughly stream order 4. The 'fast' reservoir is thus the runoff water flow that is destined for entering the 'stream' water reservoir, and implicitly represents headwater streams by filling the spatial and temporal niche between overland runoff and the river stem. "

528-540: seems like there would be less organic matter to leach from on higher slopes.

Yes, certainly an omission here. We have added in the line:

"In addition, places with higher elevation and slope in these regions tend to experience extreme cold, leading to lower NPP and so DOC leaching. "

246
247
248
249
250
251
252
253
254
255
256
257
258
259
260
261
262
263
264
265
266
267
268
269
270
271
272
273
274
275
276
277
278
279
280
281
282
283
284
285
286
287
288
289
290
291
292
293
294

Equation 2: needs units, what does 12.011 represent? A carbon unit conversion?

This has now been altered to:

"Where the pCO_2 (atm.) of a given (e.g. 'stream', 'fast', 'slow' and floodplain) water pool (pCO_{2POOL}) is given by the dissolved CO_2 concentration in that pool [$CO_{2(aq)}$], the molar weight of carbon (12.011 g mol⁻¹) and K_{CO_2} ."

Equation 3, 4, 6, ditto. If these are empirically derived parameters there needs to be a reference.

For Eq. 3 we add in the text: "Water temperature (T_{WATER} , (°C)) isn't simulated by the model, but is estimated here from the average daily surface temperature (T_{GROUND} , (°C)) in the model (Eq. 3), a derivation calculated for ORCHILEAK by Lauerwald et al. (2017) and retained here."

For Eq. 4, the Schmidt number that is calculated is entirely from Wanninkhof, and cited therein in the following segment: " With our water temperature estimate, both K_{CO_2} and the Schmidt number (Sc , Eq. 4) from Wanninkhof (1992) can be calculated, allowing for simulation of actual gas exchange velocities from standard conditions.

For Eq. 6, we follow the standard CENTURY soil carbon pool formulation (Parton et al., 1987) in which rates enter black boxes of soil carbon for each grid cell and are then re-divisible over desired quantities (area/volume etc), which is why for these we did not give units, as it is simply a discrete mass over discrete time.

More specifically, the CENTURY carbon pools, rate modifiers are determined based on soil organic dynamic in Parton et al. (1987) and then evaluated on other ecosystems (Eglin et al., 2010, Dimassi et al., 2018) for ORCHIDEE. A slightly modified version of this, with the same CENTURY parameters that now account for the priming effect, was derived by Guenet et al. (2016) and included in this version. The parameters in this equation are derived in the cited references (see Equations 1-8 in Guenet et al. 2016) and repeated in Guenet et al (2018). For clarity, we have made the following edit to the text, reflecting the fact that k is the standard decomposition rate in 1/time, the rate modifiers are zero-dimensional and SOC represents the mass of SOC, represented here by Kg as the SI unit of mass:

" Where IN_{SOC} is the carbon input to that pool, k is the SOC decomposition rate (1/dt), FOC (Kg) is a stock of matter interacting with this SOC pool to produce priming, c is a parameter controlling this interaction, SOC is the SOC reservoir (Kg), and θ , Φ and γ the zero-dimensional moisture, temperature and soil texture rate modifiers that modulate decomposition in the code, and are originally determined by the CENTURY formulation (Parton et al., 1987) and subsequently re-estimated to include priming in Guenet et al., (2016, 2018)."

Figure 1. part k. K: assumption of soil C distribution, differences between continuous and discontinuous. Don't know how well supported this is - perhaps some justification could be found in the literature.

295
296 Yes, this is only illustrative but can be found in the literature for example the top 1m of
297 soil generally is richer in carbon in continuous over discontinuous regions, with the
298 canonical snapshot of this captured by the NCSCD.

299
300 The caption has been edited to reflect this with the following: "(k) Turbation and soil
301 carbon with depth (e.g. (Hugelius et al., 2013; Tarnocai et al., 2009), (Koven et al., 2015));"

302
303 **Terminology between headwaters, tributary in figure vs. manuscript text are**
304 **confusing.**

305
306 The terminology we agree is a bit confusing because of the nomenclature that is used in
307 the model code and in preceding papers cited herein which refer to real-world water
308 pools like streams as 'fast reservoir' and real-world water pools like rivers as 'stream
309 reservoir'. However, as this figure is a cartoon, we feel it appropriate to use real-world
310 terms for bodies such as streams and tributaries that are represented collectively in the
311 model by both the 'fast' and 'stream' pool.

312
313 Thus in the caption text we include the following sentence: " Note that 'tributaries' in the
314 Figure may be represented in the model by either the 'fast' or 'stream' pool, depending on
315 their size."

316
317
318 **Author Response to Interactive Comment by Anonymous Referee #2 on**
319 **"ORCHIDEE MICT-LEAK(r5459), a global model for the production, transport and**
320 **transformation of dissolved organic carbon from Arctic permafrost regions, Part**
321 **1: Rationale, model description and simulation protocol"** by Simon P. K. Bowring
322 **et al.**

323
324 Dear Anonymous Referee #2,

325
326 Thank you for taking the time to read and review our manuscript, and in doing so
327 providing such diligent and constructive commentary for its improvement, which we
328 hope we have been able to assimilate into its content to the greatest degree possible in
329 our responses, which follow below.

330
331 **Major Comments:**

332
333 **1. All abbreviations should be spelled out at their first usage in the Abstract as**
334 **well as the main text. For instance, ORCHIDEE MICTLEAK should be spelled out in**
335 **abstract as well as the main text, where this term is first mentioned. In addition,**
336 **"IPSL", "DOC-C" and "MCT" are also not spelled out. Please check for all**
337 **abbreviations throughout the manuscript and define them at the first usage.**

338
339 1. We have included the full expansion of the acronyms identified by your review and
340 included them in the main body of the text. In the abstract, we have included the full
341 spelling of 'IPSL' (Institut Pierre Simon Laplace), to reflect the fact that this may not be a
342 well-known institute, but have decided not to do the same for 'ORCHIDEE' in the
343 abstract, as (i) this is a relatively well-known land surface model in the modelling

344 [community, such that it may not be necessary to unpack its letters in an abstract; \(ii\)](#)
345 [this unpacking is extremely lengthy, and may not be sufficiently informative to justify its](#)
346 [inclusion to the text body of an abstract. Thus the unpacking occurs in line 72 of the](#)
347 [text. Finally, we cannot spell out "ORCHIDEE MICT-LEAK" since the second half of the](#)
348 [compound name \(LEAK\) is itself not an acronym, and refers to a version of the](#)
349 [ORCHIDEE model called ORCHILEAK -hence our reduction of the new branch name](#)
350 [presented in this manuscript from ORCHIDEE MICT-LEAK to ORCHIDEE M-L. The](#)
351 [rationale for the ORCHILEAK name is now included in the text \(L. 81-82\) with the text "](#)
352 [where the suffix 'LEAK' holds no acronym, and refers to the 'leakage' of carbon from](#)
353 [terrestrial to aquatic realms\). "](#) Further, in the abstract we try to clarify the point that
354 [the presented model results from the merge of two separate code versions with the](#)
355 [following text: " The model, ORCHIDEE MICT-LEAK, which represents the merger of](#)
356 [previously described ORCHIDEE versions -MICT and -LEAK, mechanistically represents..."](#)

357
358 **[2. Line 46: "... as the permafrost line migrates poleward over time." is incorrect,](#)**
359 **[because there is no line in permafrost zone. However, there is boundary between](#)**
360 **[continuous and discontinuous permafrost zones, and this boundary is slowly](#)**
361 **[moving poleward over time. Please correct the phrase with respect to this](#)**
362 **[suggestion.](#)**

363
364 [2. Thank you for spotting this conceptually misleading description in our text, and for](#)
365 [providing some helpful pointers towards its resolution. The phrase has now been](#)
366 [modified to "... as the boundary between discontinuous and continuous permafrost](#)
367 [migrates poleward and toward the continental interior over time."](#)

368
369
370 **[3. Please edit English grammar throughout the manuscript more carefully. For](#)**
371 **[example, in line 70 "To this end" is not clear. In addition, in line 62 "metabolising"](#)**
372 **[should be "metabolizing".](#)**

373
374 [3. Thank you for finding this grammatical inconsistency in our text, which reflects the](#)
375 [inputs of authors using differing standards for English spelling. The GMD English](#)
376 [language guidelines stipulate that "We accept all standard varieties of English in order to](#)
377 [retain the author's voice. However, the variety should be consistent within each article". As](#)
378 [such, we have chosen to homogenise the text for the UK variant. Thus 'metabolize' and](#)
379 [its variants have now all been corrected to reflect this choice of English usage in the](#)
380 [other text \(e.g. lines 125-126\), as have all other verbs that contain this \('-z'\) difference in](#)
381 [spelling \(e.g. 'mineralization' --> 'mineralisation', line 461\) throughout the text.](#)
382 [Further, "to this end" has been changed to "for this purpose".](#)

383 **[Minor Comments:](#)**

384
385
386 **[1. Lines 50-51: "... , the majority as dissolved organic carbon \(DOC\)." is not clear.](#)**
387 **[Please cite some references supporting the statement. For instance, in the](#)**
388 **[headwater of the Lena River basin, Suzuki et al. \(2006\) showed that DOC was a](#)**
389 **[dominant form of riverine organic carbon transport because inorganic carbon and](#)**
390 **[particulate organic carbon \(POC\) transport would be negligible on the basis of](#)**
391 **[their observation data. Suzuki, K. et al. \(2006\), Nordic Hydrology, 37\(3\), 303-312,](#)**
392 **[doi:10.2166/nh.2006.015.](#)**

393
394
395
396
397
398
399
400
401
402
403
404
405
406
407
408
409
410
411
412
413
414
415
416
417
418
419
420
421
422
423
424
425
426
427
428
429
430
431
432
433
434
435
436
437
438
439
440

Thank you for pointing out this unqualified statement. We have included the citation suggested in review.

2. Line 116-117: Please consider citing Suzuki et al. (2006).

This has been included in the text (now line 128).

3. Line 133-134: "... , and DOC concentration are affected at watershed scale by parent material and ground ice condition (O'Donnell et al., 2016)." The statement is incomplete, because DOC concentration is also affected by active layer depth as the frozen ground table limits water infiltration into deeper soil layers, as shown by Suzuki et al. (2006).

Thank you for finding this error in conceptualisation. Indeed, we agree with the reviewer that this is a critical determinant of DOC concentrations, and have altered the text to reflect this with "DOC concentrations are affected at watershed scale by parent material, ground ice content (O'Donnell et al., 2016) and active layer depth (Suzuki et al., 2006)."

4. Line 169: "... and greater evapotranspiration (Zhang et al., 2009)." Please consider adding the study by Suzuki et al. (2018), wherein they have shown increasing evapotranspiration from the entire Arctic circumpolar Tundra due to summer warming. Suzuki, K. et al. (2018), Remote Sensing, 10(3), 402, doi:<https://doi.org/10.3390/rs10030402>.

Thank you for alerting us this additional citation that further strengthens the assertions made in this portion of the text (now line 187).

5. Line 373: "..., non-conservative canopy DOC production rate of 9.2×10^{-4} g DOC-C per gram ..." is not clear. Please rewrite more clearly.

Indeed, on reflection, this sentence is not particularly straightforward and has been adapted to make what has been calculated clearer to the reader. It now reads " From this we obtain a constant tree canopy DOC production rate of 9.2×10^{-4} g DOC-C per gram of leaf biomass per day (Eq. 1). This is the same for all PFTs except those representing crops, for which this value equals 0, reflecting how at a very general level, crops are small and tend no to be characterised by high organic acid loss rates from leaves due to e.g. aphids, due to human control." (now lines 394-399).

6. Line 388: "3.5 Hydrological mobilisation of soil DOC" should be "3.5 Hydrological mobilization of soil DOC".

This has now been included (see Major Comments Response (3)).

7. Line 396: "... (see sections 'soil flooding' and 'floodplain representation')." Please add the specific section numbers.

441 [Here we realise that the section headings had changed since this part was written, and](#)
442 [we had since merged the segments discussing floodplain representation. This is now](#)
443 [reflected in the text body \(line 424\) which now reads: "\(see section 2.8, 'Representation](#)
444 [of floodplain hydrology and their DOC budget'\)."](#)

445
446 **[8. Lines 520-522: Please consider citing Suzuki et al. \(2006\), because they](#)**
447 **[observed very large DOC transport from a headwater basin of the Lena River](#)**
448 **[basin.](#)**

449 [Thank you for your suggestion. This has now been included.](#)

451
452 **[9. Line 654: "... , such as the photochemical breakdown of riverine OC, ...". Here, OC](#)**
453 **[is not clear. Please define this and add explanation.](#)**

454 [Thank you, this has been corrected to "dissolved organic carbon" \(now line 691\).](#)

455
456
457 **[10. For equations \(1\)-\(6\): within the equations, variables are in italics but variables in](#)**
458 **[the main text are in normal font. Please modify these for consistency.](#)**

459
460 [Indeed, we had not noticed this inconsistency in the text, which has now been edited](#)
461 [accordingly throughout.](#)

462
463 **[12. In Figure 1, letters \(a\)-\(m\) are too small to read. Please enlarge the letters.](#)**

464 [\(note, no 11. in the original review document\). The font size for the letter subheadings](#)
465 [has been increased from 8 point to 12 point in Figure 1.](#)

466
467
468 **[13. In the caption of Figure 1, line 1254, "\(d\) Hydrological mobilisation of soil](#)**
469 **[DOC" should be "\(d\) Hydrological mobilization of soil DOC"](#)**

470 [This remains as was \(see choice of English in Major Comments \(3\)\).](#)

471
472
473 **[14. In the caption of Figure 2, line 1277 "Blue dashed boxes" should be "Blue](#)**
474 **[colored boxes".](#)**

475
476 [This change has been included in the document.](#)

477
478
479
480
481
482
483
484
485
486
487
488
489

490
491
492
493
494
495
496
497
498
499
500
501
502
503
504
505
506
507
508
509
510
511
512
513
514
515
516
517
518
519
520
521
522
523
524
525
526
527
528
529
530
531
532
533
534
535
536
537
538

Title :

ORCHIDEE MICT-LEAK (r5459), a global model for the production, transport and transformation of dissolved organic carbon from Arctic permafrost regions, Part 1: Rationale, model description and simulation protocol.

Authors:

S.P.K. Bowring¹, R. Lauerwald², B. Guenet¹, D. Zhu¹, M. Guimberteau^{1,3}, A. Tootchi³, A. Ducharne³, P. Ciais¹

Affiliations:

[1] Laboratoire des Sciences du Climat et de l'Environnement, LSCE, CEA, CNRS, UVSQ, 91191 Gif Sur Yvette, France
[2] Department of Geoscience, Environment & Society, Université Libre de Bruxelles, 1050 Bruxelles, Belgium
[3] Sorbonne Université, CNRS, EPHE, Milieux environnementaux, transferts et interaction dans les hydrosystèmes et les sols, Metis, 75005 Paris, France

Abstract

Few Earth System models adequately represent the unique permafrost soil biogeochemistry and its respective processes; this significantly contributes to uncertainty in estimating their responses, and that of the planet at large, to warming. Likewise, the riverine component of what is known as the 'boundless carbon cycle' is seldom recognised in Earth System modelling. Hydrological mobilisation of organic material from a ~1330–1580 PgC carbon stock to the river network results either in sedimentary settling or atmospheric 'evasion', processes widely expected to increase with amplified Arctic climate warming. Here, the production, transport and atmospheric release of dissolved organic carbon (DOC) from high-latitude permafrost soils into inland waters and the ocean is explicitly represented for the first time in the land surface component (ORCHIDEE) of a CMIP6 global climate model (Institut Pierre Simon Laplace (IPSL)). The model, ORCHIDEE MICT-LEAK, which represents the merger of previously described ORCHIDEE versions -MICK and -LEAK, mechanistically represents (a) vegetation and soil physical processes for high latitude snow, ice and soil phenomena, and (b) the cycling of DOC and CO₂, including atmospheric evasion, along the terrestrial-aquatic continuum from soils through the river network to the coast, at 0.5° to 2° resolution. This paper, the first in a two-part study, presents the rationale for including these processes in a high latitude specific land surface model, then describes the model with a focus on novel process implementations, followed by a summary of the model configuration and simulation protocol. The results of these simulation runs, conducted for the Lena River basin, are evaluated against observational data in the second part of this study.

1 Introduction

High-latitude permafrost soils contain large stores of frozen, often ancient and relatively reactive carbon up to depths of over 30m. Soil warming caused by contemporary anthropogenic climate change can be expected to destabilise these stores (Schuur et al., 2015), via microbial or hydrological mobilisation following spring/summer thaw and riverine discharge (Vonk et al., 2015a) as the boundary between discontinuous and

Simon Bowring 31/5/y 12:21
Mis en forme: Vérifier l'orthographe et la grammaire

Simon Bowring 31/5/y 12:21
Mis en forme: Vérifier l'orthographe et la grammaire

Simon Bowring 31/5/y 12:21
Mis en forme: Anglais (G.B.), Vérifier l'orthographe et la grammaire

Simon Bowring 31/5/y 12:21
Mis en forme: Vérifier l'orthographe et la grammaire

Simon Bowring 30/5/y 15:32
Supprimé: z

Simon Bowring 31/5/y 12:21
Mis en forme: Vérifier l'orthographe et la grammaire

Simon Bowring 30/5/y 15:32
Supprimé: z

Simon Bowring 5/6/y 15:44
Supprimé:

Simon Bowring 31/5/y 12:21
Mis en forme: Vérifier l'orthographe et la grammaire

Simon Bowring 31/5/y 12:21
Mis en forme: Vérifier l'orthographe et la grammaire

Simon Bowring 30/5/y 15:33
Supprimé: z

Simon Bowring 31/5/y 12:21
Mis en forme: Vérifier l'orthographe et la grammaire

Simon Bowring 30/5/y 15:33
Supprimé: z

Simon Bowring 31/5/y 12:21
Mis en forme: Vérifier l'orthographe et la grammaire

Simon Bowring 3/6/y 10:35
Mis en forme: Police :Non Italique

544 [continuous permafrost migrates poleward and toward the continental interior over](#)
545 [time.](#) The high latitude soil carbon reservoir may amount to ~1330–1580 PgC
546 (Hugelius et al., 2013, 2014; Tarnocai et al., 2009), –over double that stored in the
547 contemporary atmosphere, while [the yearly lateral flux of carbon from soils to running](#)
548 [waters may amount to about a fifth of net ecosystem carbon exchange \(~400 TgC yr⁻¹\),](#)
549 [about ~40% of which may be contributed by DOC \(McGuire et al., 2009\).](#) Excluding the
550 [dissolved inorganic carbon component of this flux, as well as dissolved CO₂ input from](#)
551 [soils, the vast majority \(85%\) of riverine organic carbon transfer to the Arctic Ocean](#)
552 [occurs as dissolved organic carbon \(DOC\), as described in \(e.g.\) Suzuki et al. \(2006\).](#)

553
554 The fact that, to our knowledge, no existing land surface models are able to adequately
555 simultaneously represent this unique high latitude permafrost soil environment, the
556 transformation of soil organic carbon (SOC) to its eroded particulate and DOC forms and
557 their subsequent lateral transport, as well as the response of all these to warming,
558 entails significant additional uncertainty in projecting global-scale biogeochemical
559 responses to human-induced environmental change.

560
561 Fundamental to these efforts is the ability to predict the medium under which carbon
562 transformation will occur: in the soil, streams, rivers or sea, and under what
563 metabolising conditions –since these will determine the process mix that will ultimately
564 enable either terrestrial redeposition and retention, ocean transfer, or atmospheric
565 release of permafrost-derived organic carbon. In the permafrost context, this implies
566 being able to accurately represent (i) the source, reactivity and transformation of
567 released organic matter, and; (ii) the dynamic response of hydrological processes to
568 warming, since water phase determines carbon, heat, and soil moisture availability for
569 metabolism and lateral transport.

570
571 [For this purpose](#), we take a specific version of the terrestrial component of the [Institut](#)
572 [Pierre Simon Laplace \(IPSL\)](#) global Earth System model (ESM) ORCHIDEE (Organising
573 Carbon and Hydrology In Dynamic Ecosystems), one that is specifically coded for,
574 calibrated with and evaluated on high latitude phenomena and permafrost processes,
575 called ORCHIDEE-MICT ([where MICT stands for aMeliorated Interactions between](#)
576 [Carbon and Temperature](#) (Guimberteau et al., 2018)). This code is then adapted to
577 include DOC production in the soil (ORCHIDEE-SOM, (Camino-Serrano et al., 2018)),
578 ‘priming’ of SOC (ORCHIDEE-PRIM, (Guenet et al., 2016, 2018)) and the riverine
579 transport of DOC and CO₂, including in-stream transformations, carbon and water
580 exchanges with wetland soils and gaseous exchange between river surfaces and the
581 atmosphere (ORCHILEAK (Lauerwald et al., 2017), [where the suffix 'LEAK' holds no](#)
582 [acronym, and refers to the 'leakage' of carbon from terrestrial to aquatic realms](#)).

583
584 The resulting model, dubbed ORCHIDEE MICT-LEAK, hereafter referred to as MICT-L for
585 brevity, is therefore able to represent: (a) Permafrost soil and snow physics,
586 thermodynamics to a depth of 38m and dynamic soil hydrology to a depth of 2m; (b)
587 Improved representation of biotic stress response to cold, heat and moisture in high
588 latitudes; (c) Explicit representation of the active layer and frozen-soil hydrologic
589 barriers; buildup of soil carbon stocks via primary production and vertical translocation
590 (turbation) of SOC and DOC; (d) DOC leaching from tree canopies, atmospheric
591 deposition, litter and soil organic matter, its adsorption/desorption to/from soil
592 particles, its transport and transformation to dissolved CO₂ (CO_{2(aq)}) and atmospheric

Simon Bowring 31/5/y 12:21
Mis en forme: Vérifier l'orthographe et la grammaire

Simon Bowring 30/5/y 15:20
Supprimé: as the permafrost line migrates poleward over time. ... [1]

Simon Bowring 31/5/y 12:21
Mis en forme ... [2]

Unknown
Code de champ modifié

Simon Bowring 3/6/y 09:59
Mis en forme ... [3]

Simon Bowring 31/5/y 11:36
Supprimé: the yearly lateral flux of carbon from soils to running waters may amount to ~40% of net ecosystem carbon exchange (McGuire et al., 2009), the majority as dissolved organic carbon (DOC)

Unknown
Code de champ modifié

Simon Bowring 3/6/y 09:59
Mis en forme ... [4]

Simon Bowring 3/6/y 09:59
Mis en forme ... [5]

Simon Bowring 31/5/y 12:32
Supprimé: s

Simon Bowring 30/5/y 16:46
Supprimé: To this end

Simon Bowring 31/5/y 12:21
Mis en forme ... [6]

Simon Bowring 30/5/y 14:51
Supprimé: (Lauerwald et al., 2017)

Simon Bowring 31/5/y 12:21
Mis en forme ... [7]

Simon Bowring 31/5/y 12:21
Mis en forme: Vérifier l'orthographe et la grammaire

614 release, as well as the production and hydrological transport of plant root-zone derived
615 dissolved CO₂; (e) Improved representation of C cycling on floodplains; (f) Priming of
616 organic matter in the soil column and subsequent decomposition dynamics. In
617 combination, these model properties allow us to explore the possibility of reproducing
618 important emergent phenomena observed in recent empirical studies (Fig. 1) arising
619 from the interaction of a broad combination of different processes and factors.

620
621 To our knowledge very few attempts have been made at the global scale of modelling
622 DOC production and lateral transfer from the permafrost region that explicitly accounts
623 for such a broad range of high latitude-specific processes, which in turn allows us to
624 match and evaluate simulation outputs with specific observed processes, enhancing our
625 ability to interpret the output from these models and improve our understanding of the
626 processes represented. The only other attempt at doing so is a Pan-Arctic modelling
627 study by Kicklighter et al. (2013), which is based on a relatively simplified scheme for
628 soil, water and biology. The following segment briefly overviews the dynamics,
629 emergent properties and their overall significance across scales, of permafrost region
630 river basins.

631 ***A giant, reactive, fast-draining funnel: A permafrost basin overview***

632 Permafrost has a profound impact on Arctic river hydrology. In permafrost regions, a
633 permanently frozen soil layer acts as a 'cap' on ground water flow (see 'permafrost
634 barrier', right hand side of Fig. 1). This implies that: (i) Near-surface runoff becomes by
635 far the dominant flowpath draining permafrost watersheds (Ye et al., 2009), as shown
636 in Fig. 1d; (ii) The seasonal amplitude of river discharge, expressed by the ratio of
637 maximum to minimum discharge ($Q_{\max:\min}$ in Fig. 1), over continuous versus
638 discontinuous permafrost catchments is higher as a result of the permafrost barrier;
639 (iii) This concentration of water volume near the surface causes intense leaching of DOC
640 from litter and relevant unfrozen soil layers (Fig. 1g, 1d, e.g. Suzuki et al., 2006) Drake
641 et al., (2015); Spencer et al., (2015); (Vonk et al., (2015a,b)); (iv) Permafrost SOC stocks
642 beneath the active layer are physically and thermally shielded from aquatic mobilisation
643 and metabolisation, respectively (Fig. 1g).

644
645
646
647 Rapid melting of snow and soil or river ice during spring freshet (May-June) drives
648 intensely seasonal discharge, with peaks often two orders of magnitude (e.g. Van Vliet et
649 al., (2012)) above baseflow rates (Fig. 1d). These events are the cause of four, largely
650 synchronous processes: (i) Biogenic matter is rapidly transported from elevated
651 headwater catchments (Fig. 1, right hand side) (McClelland et al., 2016); (ii) Plant
652 material at the soil surface is intensely leached, with subsequent mobilisation and
653 transformation of this dissolved matter via inland waters (Fig. 1d,b,j); During spring
654 freshet, riverine DOC concentrations increase and bulk annual marine DOC exports are
655 dominated by the terrestrial DOC flux to the rivers that occurs at this time (Holmes et al.,
656 2012). Indeed, DOC concentrations during the thawing season tend to be greater than
657 or equal to those in the Amazon particularly in the flatter Eurasian rivers (Holmes et al.,
658 2012; McClelland et al., 2012), and DOC concentrations are affected at watershed scale
659 by parent material, ground ice content (O'Donnell et al., 2016) and active layer depth
660 (Suzuki et al., 2006).

661

Simon Bowring 31/5/y 12:21
Mis en forme ... [8]

Simon Bowring 31/5/y 12:21
Mis en forme ... [9]

Simon Bowring 31/5/y 12:21
Mis en forme ... [10]

Simon Bowring 31/5/y 12:21
Mis en forme ... [11]

Simon Bowring 31/5/y 12:21
Mis en forme ... [12]

Simon Bowring 31/5/y 12:21
Mis en forme ... [13]

Simon Bowring 30/5/y 16:00
Supprimé: (

Simon Bowring 31/5/y 12:21
Mis en forme ... [14]

Simon Bowring 31/5/y 12:21
Mis en forme ... [15]

Simon Bowring 31/5/y 12:21
Mis en forme ... [16]

Simon Bowring 31/5/y 12:21
Mis en forme ... [17]

Simon Bowring 31/5/y 12:21
Mis en forme ... [18]

Simon Bowring 30/5/y 15:22
Supprimé: z

Simon Bowring 30/5/y 15:22
Supprimé: z

Simon Bowring 31/5/y 12:21
Mis en forme ... [19]

Simon Bowring 31/5/y 12:21
Mis en forme ... [20]

Simon Bowring 31/5/y 12:21
Mis en forme ... [21]

Simon Bowring 31/5/y 12:21
Mis en forme ... [22]

Simon Bowring 30/5/y 15:33
Supprimé: z

Simon Bowring 31/5/y 12:21
Mis en forme ... [23]

Simon Bowring 31/5/y 12:21
Mis en forme ... [24]

Simon Bowring 30/5/y 16:02
Supprimé: and

Simon Bowring 31/5/y 12:21
Mis en forme ... [25]

Simon Bowring 31/5/y 12:21
Mis en forme ... [26]

Simon Bowring 31/5/y 12:21
Mis en forme ... [27]

Simon Bowring 31/5/y 12:21
Mis en forme ... [28]

667 (iii) Sudden inundation of the floodplain regions in spring and early summer (Fig. 1h),
668 (Smith and Pavelsky, 2008), further spurs lateral flux of both particulate and dissolved
669 matter in the process and its re-deposition (Zubrzycki et al., 2013), or atmospheric
670 evasion (Fig. 1j,m); (iv) Snowmelt-induced soil water saturation, favouring the growth of
671 moss and sedge-based ecosystems (e.g. Selvam et al., 2017; Tarnocai et al., 2009; Yu,
672 2011), and the retention of their organic matter (OM), i.e., peat formation, not shown in
673 Fig. 1 as this isn't represented in this model version, but is generated in a separate
674 branch of ORCHIDEE (Qiu et al., 2018)).

676 Mid-summer river low-flow and a deeper active layer allow for the hydrological
677 intrusion and leaching of older soil horizons (e.g. the top part of Pleistocene-era Yedoma
678 soils), and their subsequent dissolved transport (e.g. Wickland et al., 2018). These
679 sometimes-ancient low molecular weight carbon compounds appear to be preferentially
680 and rapidly metabolised by microbes in headwater streams (Fig. 1j), which may
681 constitute a significant fraction of aggregate summer CO₂ evasion in Arctic rivers
682 (Denfeld et al., 2013; Vonk et al., 2015). This is likely due to the existence of a significant
683 labile component of frozen carbon (Drake et al., 2015; Vonk et al., 2013; Woods et al.,
684 2011);

686 CO₂ evasion rates from Arctic inland waters (Fig. 1j,e,m), which include both lakes and
687 rivers, are estimated to be 40-84 TgC yr⁻¹ (McGuire et al., 2009), of which 15-30 TgC yr⁻¹
688 or one-third of the total inland evasion flux, is thought to come from rivers. Recent geo-
689 statistically determined estimates of boreal lake annual emissions alone now stands at
690 74-347 TgC yr⁻¹ (Hastie et al., 2018), although this is likely a substantial overestimate
691 (Bogard et al., 2019), which potentially lowers the riverine fraction of total CO₂ evasion.
692 These numbers should be compared with estimates of Pan-Arctic DOC discharge from
693 rivers of 25-36 TgC yr⁻¹ (Holmes et al., 2012; Raymond et al., 2007). The subsequent
694 influx of terrestrial carbon to the shelf zone is thought to total 45-54 TgC yr⁻¹. Rivers
695 supply the Arctic Ocean an estimated 34 Tg of carbon-equivalent DOC (DOC-C) yr⁻¹
696 (Holmes et al., 2012), while depositing 5.8 Tg yr⁻¹ of particulate carbon, these being
697 sourced from those rivers draining low and high elevation headwaters, respectively
698 (McClelland et al., 2016). These dynamics are all subject to considerable amplification
699 by changes in temperature and hydrology (e.g. Drake et al., 2015; Frey and McClelland,
700 2009; Tank et al., 2018).

702 Average annual discharge in the Eurasian Arctic rivers has increased by at least 7%
703 between 1936-1999 (Peterson et al., 2002), driven by increasing temperatures and
704 runoff (Berezovskaya et al., 2005), and the subsequent interplay of increasing annual
705 precipitation, decreasing snow depth and snow water equivalent (SWE) mass (Kunkel et
706 al., 2016; Mudryk et al., 2015), and greater evapotranspiration (Suzuki et al., 2018;
707 Zhang et al., 2009). Although net discharge trend rates over N. America were negative
708 over the period 1964-2003, since 2003 they have been positive on average (Dery et al.,
709 2016). These dynamic and largely increasing hydrologic flux trends point towards
710 temperature and precipitation -driven changes in the soil column, in which increased
711 soil water/snow thaw and microbial activity (Graham et al., 2012; MacKelprang et al.,
712 2011; Schuur et al., 2009), converge to raise soil leaching and DOC export rates to the
713 river basin and beyond (e.g. Vonk et al., (2015b)). Further, microbial activity generates
714 its own heat, which incubation experiments have shown may be sufficient to
715 significantly warm the soil further (Hollesen et al., 2015), in a positive feedback.

Simon Bowring 31/5/y 12:21
Mis en forme ... [29]

Simon Bowring 31/5/y 12:21
Mis en forme ... [30]

Simon Bowring 30/5/y 15:24
Supprimé: z

Simon Bowring 31/5/y 12:21
Mis en forme ... [31]

Simon Bowring 5/6/y 11:24
Mis en forme ... [32]

Simon Bowring 5/6/y 11:24
Supprimé: CO₂ evasion rates from Arctic inland waters (Fig. 1j,e,m) are estimated to be in the region of 40-84 TgC yr⁻¹ (McGuire et al., 2009), to be compared with estimates of Pan Arctic DOC discharge from rivers of 25-36 TgC yr⁻¹.

Simon Bowring 31/5/y 12:21
Mis en forme ... [33]

Simon Bowring 31/5/y 10:27
Supprimé: (Holmes et al., 2012; Raymond et al., 2007)

Simon Bowring 31/5/y 12:21
Mis en forme ... [34]

Simon Bowring 31/5/y 11:50
Supprimé: (A0)

Simon Bowring 31/5/y 12:21
Mis en forme ... [35]

Simon Bowring 5/6/y 11:29
Supprimé: (e.g. Frey et al., 2009; Drake et al., 2015; Tank et al., 2018).

Simon Bowring 31/5/y 12:21
Mis en forme ... [36]

Simon Bowring 31/5/y 12:21
Mis en forme ... [37]

740
741
742
743
744
745
746
747
748
749
750
751
752
753
754
755
756
757
758
759
760
761
762
763
764
765
766
767
768
769
770
771
772
773
774
775
776
777
778
779
780
781
782
783
784
785
786
787
788

Arctic region fire events are also on the rise and likely to increase with temperature and severity over time (Ponomarev et al., 2016). The initial burning of biomass is accompanied by active layer deepening, priming of deeper soil horizons (De Baets et al., 2016), and a significant loading of pyrogenic DOC in Arctic watersheds, up to half of which is rapidly metabolised (Myers-Pigg et al., 2015).

In these contexts, the implications of (polar-amplified) warmer temperatures leading to active layer deepening towards the future (transition from Continuous to Discontinuous Permafrost, as shown in the upper/lower segments of Fig. 1) are clear and unique: potentially sizeable aquatic mobilisation and microbial metabolism (Xue, 2017) of dissolved and eroded OM, deeper hydrological flow paths, an increase in total carbon and water mass and heat transfer to the aquatic network and, ultimately, the Arctic Ocean and atmosphere (Fig. 1i).

The advantage of having a terrestrial model that can be coupled to a marine component of an overarching global climate model (GCM) is in this case the representation of a consistent transboundary scheme, such that output from one model is integrated as input to another. This is particularly important given the context in which these terrestrial outflows occur :

Because of its small size, a uniquely large and shallow continental shelf, the global climatological significance of its seasonal sea ice (Rhein et al., 2013) and its rapid decline (Findlay et al., 2015), the [Arctic Ocean](#) has been described as a giant estuary (McClelland et al., 2012), acting as a funnel for the transport, processing and sedimentation of terrestrial OM. Because of its small surface area and shallow seas (Jakobsson, 2002), the [Arctic Ocean](#) holds relatively little volume and is consequently sensitive to inputs of freshwater, heat, alkalinity and nutrients that flush out from terrestrial sources, particularly at discharge peak.

High suspended particle loads in river water as they approach the mouth (Heim et al., 2014), cause lower light availability and water albedo and hence higher temperatures (Bauch et al., 2013; Janout et al., 2016), which can affect the near-shore sea ice extent, particularly in spring (Steele and Ermold, 2015). Volumes of riverine freshwater and total energy flux (Lammers et al., 2007), are expected to increase with warmer temperatures, along with an earlier discharge peak (Van Vliet et al., 2012, 2013). In doing so, freshwaters may in the future trigger earlier onset of ice retreat (Stroeve et al., 2014; Whitefield et al., 2015) via a freshwater albedo, ice melt, seawater albedo, ice melt, feedback, amplified by intermediary state variables such as water vapour and cloudiness (Serreze and Barry, 2011).

Both terrestrially-exported and older shelf carbon in the [Arctic Ocean](#) face considerable disruption (McGuire et al., 2009; Schuur et al., 2015), from the combined effects of increased freshwater, heat, sediment, nutrient and organic carbon flows from rapidly warming Arctic river watersheds, as well as those from melting sea ice, warmer marine water temperatures and geothermal heat sources (Janout et al., 2016; Shakhova et al., 2015). Because ORCHIDEE is a sub-component of the overarching IPSL ESM, there is scope for coupling riverine outputs of water, DOC, CO_{2(aq)} and heat from the terrestrial model as input for the IPSL marine components (Fig. 1i). Nonetheless, these are not the

Simon Bowring 31/5/y 12:21
Mis en forme ... [38]

Simon Bowring 30/5/y 15:24
Supprimé: z
Simon Bowring 31/5/y 12:21
Mis en forme ... [39]

Simon Bowring 30/5/y 15:33
Supprimé: z...tion and microbial ... [40]
Simon Bowring 31/5/y 12:21
Mis en forme ... [41]

Simon Bowring 31/5/y 12:21
Mis en forme ... [42]

Simon Bowring 31/5/y 11:49
Supprimé: A0

Simon Bowring 31/5/y 12:21
Mis en forme ... [43]

Simon Bowring 31/5/y 11:49
Supprimé: A0

Simon Bowring 31/5/y 12:21
Mis en forme ... [44]

Simon Bowring 31/5/y 11:49
Supprimé: A0

Simon Bowring 31/6/y 17:29
Mis en forme ... [45]

Simon Bowring 31/5/y 12:32
Supprimé:

802 objectives of the present paper, whose aim is rather to validate the simulated variable
803 output produced by the model described in detail below against observations and
804 empirical knowledge for the Lena basin, but are included here descriptively to scope the
805 plausible future applications of ORCHIDEE MICT-LEAK, given our present empirical
806 understanding of their potential significance. [The choice of the Lena River basin in
807 Eastern Siberia as the watershed of study for model evaluation owes itself to its size, the
808 presence of floodplains and mountain areas which allow us to test the model behavior
809 for contrasting topography, the relatively low impact of damming on the river, given that
810 ORCHIDEE only simulates undammed fluvial 'natural flow', and its mixture of
811 continuous and discontinuous permafrost with tundra grassland in the north and boreal
812 forests in the south, and is described in greater detail in Part 2 of this study.](#)

814 The Methods section summarises the model structure and associated rationale for each
815 of the model sub-branches or routines relevant to this study, and follows with the setup
816 and rationale for the simulations carried out as validation exercises.

818 2 Methods

819
820 This section overviews the processes represented in the model being described in this
821 manuscript, which is referred to as ORCHIDEE MICT-LEAK, hereafter referred to MICT-L
822 for brevity. MICT-L is at its heart a merge of two distinct models : the high-latitude land
823 surface component of the IPSL Earth System Model ORCHIDEE MICT, and the DOC-
824 production and transport branch of ORCHIDEE's default or 'trunk' version (Krinner et
825 al., 2005), ORCHILEAK. The original merger of these two code sets was between
826 ORCHILEAK and ORCHIDEE-MICT, which are described in Camino-Serrano et al.
827 (2018), Lauerwald et al. (2017), and Guimberteau et al. (2018), respectively.

829 However, [numerous improvements in code performance](#) and process additions post-
830 dating these publications have been included in this code. Furthermore, novel processes
831 included in neither of these two core models are added to MICT-L, such as the diffusion
832 of DOC through the soil column to represent its turbation and preferential stabilisation
833 at depth in the soil, [as described in Section 2.11.](#)

835 In terms of code architecture, the resulting model is substantially different from either
836 of its parents, owing to the fact that the two models were developed on the basis of
837 ORCHIDEE trunk revisions 2728 and 3976 for ORCHILEAK and MICT respectively, which
838 have a temporal model development distance of over 2 years, and subsequently evolved
839 in their own directions. These foundational differences, which mostly affect the
840 formulation of soil, carbon and hydrology schemes, mean that different aspects of each
841 are necessarily forced into the subsequent code. Where these differences were
842 considered scientific or code improvements, they were included in the resulting scheme.
843 Despite architectural novelties introduced, MICT-L carries with it a marriage of much
844 the same schemes detailed exhaustively in Guimberteau et al. (2018), and Lauerwald et
845 al. (2017). As such, the following model description details only new elements of the
846 model, those that are critical to the production and transport of DOC from permafrost
847 regions, and parameterisations specific to this study (Fig. 2).

849 2.1 Model Description

850

- Simon Bowring 3/6/y 17:29
Mis en forme: Police :Non Italique
- Simon Bowring 3/6/y 17:29
Mis en forme: Police :Non Italique
- Simon Bowring 3/6/y 17:29
Mis en forme: Police :Non Italique
- Simon Bowring 3/6/y 17:29
Mis en forme: Police :Non Italique
- Simon Bowring 3/6/y 17:29
Mis en forme: Vérifier l'orthographe et la grammaire
- Simon Bowring 31/5/y 12:21
Mis en forme: Vérifier l'orthographe et la grammaire
- Simon Bowring 31/5/y 12:21
Mis en forme: Vérifier l'orthographe et la grammaire
- Simon Bowring 31/5/y 12:21
Mis en forme: Vérifier l'orthographe et la grammaire
- Simon Bowring 31/5/y 12:21
Mis en forme: Vérifier l'orthographe et la grammaire
- Simon Bowring 31/5/y 12:21
Mis en forme ... [46]
- Simon Bowring 31/5/y 12:21
Mis en forme ... [47]
- Simon Bowring 31/5/y 12:21
Mis en forme ... [48]
- Simon Bowring 5/6/y 14:11
Supprimé: numerous bug fixes
- Simon Bowring 31/5/y 12:21
Mis en forme ... [49]
- Simon Bowring 31/5/y 12:21
Mis en forme ... [50]
- Simon Bowring 31/5/y 11:52
Supprimé: in response to phenom ... [51]
- Simon Bowring 31/5/y 11:53
Supprimé: (novel in ORCHIDEE-MICT)
- Simon Bowring 31/5/y 11:53
Supprimé: , in a process not neces ... [52]
- Simon Bowring 31/5/y 11:59
Supprimé: [53]
- Simon Bowring 31/5/y 12:21
Mis en forme ... [54]
- Simon Bowring 31/5/y 12:21
Mis en forme ... [55]
- Simon Bowring 31/5/y 12:21
Mis en forme ... [56]
- Simon Bowring 31/5/y 12:21
Mis en forme ... [57]

862 MICT-L is based largely on ORCHIDEE-MICT, into which the DOC production, transport
863 and transformation processes developed in the ORCHILEAK model version and tested
864 insofar only for the Amazon, have been transplanted, allowing for these same processes
865 to be generated in high latitude regions with permafrost soils and a river flow regime
866 dominated by snow melt. The description that ensues roughly follows the order of the
867 carbon and water flow chain depicted in Fig. 2b. At the heart of the scheme is the
868 vegetative production of carbon, which occurs along a spectrum of 13 plant functional
869 types (PFTs) that differ from one another in terms of plant physiological and
870 phenological uptake and release parameters (Krinner et al., 2005). Together, these
871 determine grid-scale net primary production. In the northern high latitudes, the boreal
872 trees (PFTs 7-9) and C3 grasses (PFT 10) dominate landscape biomass and primary
873 production. Thus, in descending order yearly primary production over the Lena basin is
874 roughly broken down between C3 grasses (48%), boreal needleleaf summergreen trees
875 (27%), boreal needleleaf evergreen trees (12%), boreal broadleaf summergreen trees
876 (8%) and temperate broad-leaved evergreen trees (6%). Naturally these basin
877 aggregates are heterogeneously distributed along latitude and temperature contours,
878 with grasses/tundra dominating at the high latitudes and (e.g.) temperate broadleaf
879 trees existing only at the southern edges of the basin.

880 2.2 Biomass generation (Fig. 1a)

883 Biomass generation, consisting of foliage, roots, above and below -ground sap and heart
884 wood, carbon reserves and fruit pools in the model, results in the transfer of these
885 carbon stores to two downstream litter pools, the structural and metabolic litter (Figure
886 2b). This distinction, defined by lignin concentration of each biomass pool (Krinner et
887 al., 2005), separates the relatively reactive litter fraction such as leafy matter from its
888 less-reactive, recalcitrant counterpart (woody, 'structural' material), with the
889 consequence that the turnover time of the latter is roughly four-fold that of the former.
890 These two litter pools are further subdivided into above and below -ground pools, with
891 the latter explicitly discretised over the first two metres of the soil column, a feature first
892 introduced to the ORCHIDEE model by Camino-Serrano et al. (2014, 2018). This marks
893 a significant departure from the original litter formulation in ORCHIDEE-MICT, in which
894 the vertical distribution of litter influx to the soil carbon pool follows a prescribed root
895 profile for each PFT. This change now allows for the production of DOC from litter
896 explicitly at a given soil depth in permafrost soils.

898 2.3 DOC generation and leaching (Fig. 1b)

900 The vast majority of DOC produced by the model is generated initially from the litter
901 pools via decomposition, such that half of all of the decomposed litter is returned to the
902 atmosphere as CO₂, as defined by the microbial carbon use efficiency (CUE) -the fraction
903 of carbon assimilated versus respired by microbes post-consumption -here set at 0.5
904 following Manzoni et al. (2012). The non-respired half of the litter feeds into 'Active',
905 'Slow' and 'Passive' free DOC pools, which correspond to DOC reactivity classes in the
906 soil column [in an analogous extension to the standard CENTURY formulation](#) (Parton et
907 al., 1987). Metabolic litter contributes exclusively to the Active DOC pool, while
908 Structural litter feeds into the other two, the distribution between them dependent on
909 the lignin content of the Structural litter. The reactive SOC pools then derive directly
910 from this DOC reservoir, in that fractions of each DOC pool, defined again by the CUE, are

Simon Bowring 31/5/y 12:21
Mis en forme: Anglais (G.B.), Vérifier l'orthographe et la grammaire

Simon Bowring 31/5/y 12:21
Mis en forme: Vérifier l'orthographe et la grammaire

Simon Bowring 31/5/y 12:21
Mis en forme: Vérifier l'orthographe et la grammaire

Simon Bowring 31/5/y 12:21
Mis en forme: Vérifier l'orthographe et la grammaire

Simon Bowring 31/5/y 12:32
Supprimé: n

Simon Bowring 31/5/y 12:21
Mis en forme: Anglais (G.B.)

Simon Bowring 31/5/y 12:21
Mis en forme: Vérifier l'orthographe et la grammaire

Simon Bowring 31/5/y 12:21
Mis en forme: Vérifier l'orthographe et la grammaire

Simon Bowring 31/5/y 12:21
Mis en forme: Vérifier l'orthographe et la grammaire

Simon Bowring 31/5/y 12:21
Mis en forme: Vérifier l'orthographe et la grammaire

Simon Bowring 31/5/y 12:21
Mis en forme: Vérifier l'orthographe et la grammaire

Simon Bowring 31/5/y 12:21
Mis en forme: Vérifier l'orthographe et la grammaire

Simon Bowring 31/5/y 12:21
Mis en forme: Vérifier l'orthographe et la grammaire

Simon Bowring 31/5/y 12:21
Mis en forme: Vérifier l'orthographe et la grammaire

Simon Bowring 4/6/y 10:18
Supprimé: .

Simon Bowring 31/5/y 12:21
Mis en forme: Vérifier l'orthographe et la grammaire

913 directly transferred to three different SOC pools, while the remainder adds to the
914 heterotrophic soil respiration. Depending on clay content and bulk density of the soil, a
915 fraction of DOC is adsorbed to the mineral soil and does not take part in these reactions
916 until it is gradually desorbed when concentrations of free DOC decrease in the soil
917 column. This scheme is explained in detail in Camino-Serrano (2018). The value of the
918 fractional redistributions between free DOC and SOC after adsorption are shown in Fig.
919 2b.

921 The approximate ratio of relative residence times for the three SOC pools in our model
922 (Active:Slow:Passive) is (1:37:1618) at a soil temperature of 5°C, or 0.843 years, 31
923 yrs. and 1364 yrs. for the three pools respectively (Fig. 2b). These are based on our
924 own exploratory model runs and subsequent calculations. The residence times of the
925 active DOC pool is ~7 days (0.02 yrs.), while the slow and passive DOC pools both have a
926 residence time of ~343 days (0.94 yrs.) at that same temperature. Upon microbial
927 degradation in the model, SOC of each pool reverts either to DOC or to CO₂, the ratio
928 between these determined again by the CUE which is set in this study at 0.5 for all donor
929 pools, in keeping with the parameter configuration in Lauerwald et al., (2017) from
930 Manzoni et al. (2012). This step in the chain of flows effectively represents leaching of
931 SOC to DOC. Note that the reversion of SOC to DOC occurs only along Active-Active,
932 Slow-Slow and Passive-Passive lines in Fig. 2b, while the conversion of DOC to SOC is
933 distributed differently so as to build up a reasonable distribution of soil carbon stock
934 reactivities. Note also that the microbial CUE is invoked twice in the chain of carbon
935 breakdown, meaning that the 'effective' CUE of the SOC-litter system is approximately
936 0.25.

937 2.4 Throughfall and its DOC (Fig. 1c)

938 In MICT-L, DOC generation also occurs in the form of wet and dry atmospheric
939 deposition and canopy exudation, collectively attributed to the throughfall, i.e. the
940 amount of precipitation reaching the ground. Wet atmospheric deposition originates
941 from organic compounds dispersed in atmospheric moisture which become deposited
942 within rainfall, and are assumed here to maintain a constant concentration. This
943 concentration we take from the average of reported rainfall DOC concentrations in the
944 empirical literature measured at sites >55°N (Bergkvist and Folkesson, 1992; Clarke et
945 al., 2007; Fröberg et al., 2006; Lindroos et al., 2011; Rosenqvist et al., 2010; Starr et al.,
946 2003; Wu et al., 2010), whose value is 3 mgC L⁻¹ of rainfall. Dry DOC deposition occurs
947 through aerosol-bound organic compounds, here assumed to fall on the canopy; canopy
948 exudation refers to plant sugars exuded from the leaf surface (e.g. honey dew) or from
949 their extraction by heterotrophs such as aphids. These two are lumped together in our
950 estimates of canopy DOC generation (gDOC per g leaf carbon), which is calibrated as
951 follows.

952 We take the average total observation-based throughfall DOC flux rate per m² of forest
953 from the aforementioned literature bundle (15.7 gC m⁻² yr⁻¹) and subtract from it the
954 wet deposition component (product of rainfall over our simulation area and the rain
955 DOC content). The remainder is then the canopy DOC, which we scale to the average leaf
956 biomass simulated in a 107-year calibration run over the Lena river basin. From this we
957 obtain a constant tree canopy DOC production rate of 9.2*10⁻⁴ g DOC-C per gram of leaf
958 biomass per day (Eq. 1). This is the same for all PFTs except those representing crops.

Simon Bowring 31/5/y 12:21
Mis en forme: Anglais (G.B.), Vérifier l'orthographe et la grammaire

Simon Bowring 31/5/y 12:21
Mis en forme: Vérifier l'orthographe et la grammaire

Simon Bowring 31/5/y 12:21
Mis en forme: Vérifier l'orthographe et la grammaire

Simon Bowring 31/5/y 12:21
Mis en forme: Vérifier l'orthographe et la grammaire

Simon Bowring 31/5/y 12:21
Mis en forme: Vérifier l'orthographe et la grammaire

Simon Bowring 31/5/y 12:21
Mis en forme: Anglais (G.B.), Vérifier l'orthographe et la grammaire

Simon Bowring 31/5/y 12:21
Mis en forme: Vérifier l'orthographe et la grammaire

Simon Bowring 31/5/y 12:21
Mis en forme: Vérifier l'orthographe et la grammaire

Simon Bowring 31/5/y 12:21
Mis en forme: Vérifier l'orthographe et la grammaire

Simon Bowring 30/5/y 16:19
Supprimé: ,

Simon Bowring 30/5/y 16:19
Supprimé: to

Simon Bowring 5/6/y 15:39
Supprimé: ,

Simon Bowring 30/5/y 16:23
Supprimé: non-conservative

Simon Bowring 30/5/y 16:20
Supprimé: , except for the crop PFTs

967 for which this value equals 0, [reflecting how at a very general level, crops are small and](#)
968 [tend no to be characterised by high organic acid loss rates from leaves due to e.g. aphids,](#)
969 [due to human control](#). Note that this production of DOC should be C initially fixed by
970 photosynthesis, but it is here represented as an additional carbon flux. The dry
971 deposition of DOC through the canopy is given by:
972

$$(1) TF_{DRY} = M_{LEAF} * 9.2 * 10^{-4} \frac{dt}{day}$$

973
974 Where TF_{DRY} is dry deposition of DOC from the canopy, M_{LEAF} is leaf biomass, dt is the
975 timestep of the surface hydrology and energy balance module (30min) and day is 24
976 hours. This accumulates in the canopy and can be flushed out with the throughfall and
977 percolates into the soil surface or adds to the DOC stock of surface waters. The wet and
978 canopy deposition which hits the soil is then assumed to be split evenly between the
979 labile and refractory DOC pools (following Aitkenhead-Peterson et al., 2003).

982 2.5 Hydrological mobilisation of soil DOC (Fig. 1d)

984 All DOC pools, leached from the decomposition of either litter and SOC or being
985 throughfall inputs, reside at this point in discrete layers within the soil column, but are
986 now also available for vertical advection and diffusion, as well as lateral export from the
987 soil column as a carbon tracer, via soil drainage and runoff.
988

989 Export of DOC from the soil to rivers occurs through surface runoff, soil-bottom
990 drainage, or flooding events (see section, [2.8, 'Representation of floodplain hydrology](#)
991 [and their DOC budget'](#)). Runoff is activated when the maximum water infiltration rate of
992 the specific soil has been exceeded, meaning that water arrives at the soil surface faster
993 than it can enter, forcing it to be transported laterally across the surface. DOC is drawn
994 up into this runoff water flux from the first 5 layers of the soil column, which correspond
995 to a cumulative source depth of 4.5cm.
996

997 Drainage of DOC occurs first as its advection between the discrete soil layers, and its
998 subsequent export from the 11th layer, which represents the bottom of the first 2m of
999 the soil column, from which export is calculated as a proportion of the DOC
1000 concentration at this layer. Below this, soil moisture and DOC concentrations are no
1001 longer explicitly calculated, except in the case that they are cryoturbated below this, up
1002 to a depth of 3m. DOC drainage is proportional to but not a constant multiplier of the
1003 water drainage rate for two reasons. [First, as it water percolates through the soil](#)
1004 [column, it carries DOC along from one layer to another through the entirety of the soil](#)
1005 [column, but this percolation is blocked when the soil is entirely frozen, i.e. it is assumed](#)
1006 [that all soil pores are filled with ice which blocks percolation. This implies that DOC](#)
1007 [transport is not just determined by what enters from the top but also by the below](#)
1008 [ground production from litter, the sorption and de-sorption to and from particulate soil](#)
1009 [organic carbon in the soil column, its decomposition within the soil column, and water](#)
1010 [vertical transport entraining DOC between the non-frozen soil layers using the hydraulic](#)
1011 [conductivity calculated by the model as a function of soil texture, soil carbon and time-](#)
1012 [dependent soil moisture \(Guimberteau et al., 2018\).](#)
1013

Simon Bowring 31/5/y 12:21

Mis en forme

... [58]

Simon Bowring 31/5/y 12:21

Mis en forme

... [59]

Simon Bowring 31/5/y 12:21

Mis en forme: Vérifier l'orthographe et la grammaire

Simon Bowring 30/5/y 16:27

Supprimé: s

Simon Bowring 31/5/y 12:21

Mis en forme: Police :Non Gras, Vérifier l'orthographe et la grammaire

Simon Bowring 30/5/y 16:27

Supprimé: 'soil flooding' and 'floodplain representation'

Simon Bowring 31/5/y 12:21

Mis en forme: Vérifier l'orthographe et la grammaire

Simon Bowring 3/6/y 10:09

Mis en forme: Justifié

Simon Bowring 5/6/y 10:51

Mis en forme

... [60]

1020 Secondly, in order to account for preferential flow paths in the soil created by the
1021 subsoil actions of flora and fauna, and for the existence of non-homogenous soil textures
1022 at depth that act as aquitards, DOC infiltration must account for the fact that area-
1023 aggregated soils drain more slowly, increasing the residence time of DOC in the soil.
1024 Thus a reduction factor which reduces the vertical advection of DOC in soil solution by
1025 80% compared to the advection is applied to represent a slow down in DOC percolation
1026 through the soil and increase its residence time there.

Simon Bowring 31/5/y 12:41
Supprimé: First, in the process of drainage DOC is able to percolate from one layer to another, through the entirety of the soil column, meaning that vertical transport is not solely determined by 11th layer concentrations, given that DOC can be continuously leached and transported over the whole soil column.
Simon Bowring 31/5/y 12:21
Mis en forme ... [61]

1028 In MICT-L, as in ORCHILEAK, a 'poor soils' module reads off from a map giving fractional
1029 coverage of land underlain by Podzols and Arenosols at the 0.5° grid-scale, as derived
1030 from the Harmonized World Soil Database (Nachtergaele, 2010). Due to their low pH
1031 and nutrient levels, areas identified by this soil-type criterion experience soil organic
1032 matter decomposition rates half that of other soils (Lauerwald et al. (2017), derived
1033 from Bardy et al. (2011); Vitousek & Sanford (1986); Vitousek & Hobbie (2000)). To
1034 account for the very low DOC-filtering capacity of these coarse-grained, base- and clay-
1035 poor soils (DeLuca & Boisvenue (2012), Fig. 2b), no reduction factor in DOC advection
1036 rate relative to that of water in the soil column is applied when DOC is generated within
1037 these "poor soils".

Simon Bowring 31/5/y 12:21
Mis en forme ... [62]

1039 By regulating both decomposition and soil moisture flux, the "poor soil" criterion
1040 effectively serves a similar if not equal function to a soil 'tile' for DOC infiltration in the
1041 soil column (inset box of Fig. 1), because soil tiles (forest, grassland/tundra/cropland
1042 and bare soil) are determinants of soil hydrology which affects moisture-limited
1043 decomposition. Here however, the 'poor soil' criteria is applied uniformly across the
1044 three soil tiles of each grid cell. This modulation in MICT-L is of significance for the
1045 Arctic region, given that large fractions of the discontinuous permafrost region are
1046 underlain by Podzols, particularly in Eurasia. For the Arctic as a whole, Podzols cover
1047 ~15% of total surface area (DeLuca and Boisvenue, 2012). Further, in modelled frozen
1048 soils, a sharp decline in hydraulic conductivity is imposed by the physical barrier of ice
1049 filling the soil pores, which retards the flow of water to depth in the soil, imposing a cap
1050 on drainage and thus potentially increasing runoff of water laterally, across the soil
1051 surface (Gouttevin et al., 2012). In doing so, frozen soil layers overlain by liquid soil
1052 moisture will experience enhanced residence times of water in the carbon-rich upper
1053 soil layers, potentially enriching their DOC load. Note that ice wedges, an important
1054 component of permafrost landscapes and their thaw processes, are not included in the
1055 current terrestrial representation, but have been previously simulated in other models
1056 (Lee et al., 2014).

Simon Bowring 31/5/y 12:15
Supprimé: .

Simon Bowring 31/5/y 12:16
Supprimé: ecah

Simon Bowring 31/5/y 12:21
Mis en forme ... [63]

Simon Bowring 3/6/y 10:11
Supprimé:

Simon Bowring 31/5/y 12:21
Mis en forme ... [64]

1058 Thus, for all the soil layers in the first 2m, DOC stocks are controlled by production from
1059 litter and SOC decay, their advection, diffusion, and consumption by DOC mineralisation,
1060 as well as buffering by adsorption and desorption processes.

Simon Bowring 31/5/y 12:21
Mis en forme: Anglais (G.B.)

Simon Bowring 30/5/y 15:25
Supprimé: z

Simon Bowring 31/5/y 12:21
Mis en forme: Vérifier l'orthographe et la grammaire

Simon Bowring 3/6/y 17:28
Mis en forme ... [65]

1062 2.6 Routing Scheme:

1064 The routing scheme in ORCHIDEE, first described in detail in Ngo-Duc et al. (2007) and
1065 presented after some version iterations in Guimberteau et al. (2012), is the module
1066 which when activated, represents the transport of water collected by the runoff and
1067 drainage simulated by the model along the prescribed river network in a given
1068 watershed. In doing so, its purpose is to coarsely represent the hydrologic coupling

1093 between precipitation inputs to the model and subsequent terrestrial runoff and
1094 drainage (or evaporation) calculated by it on the one hand, and the eventual discharge of
1095 freshwater to the marine domain, on the other. In other words, the routing scheme
1096 simulates the transport of water by rivers and streams, by connecting rainfall and
1097 continental river discharge with the land surface.
1098

1099 To do so, the routing scheme first inputs a map of global watersheds at the 0.5 degree
1100 scale (Oki et al., 1999; Vorosmarty et al., 2000), which gives watershed and sub-basin
1101 boundaries and the direction of water-flow based on topography to the model. The
1102 water flows themselves are comprised of three distinct linear reservoirs within each
1103 sub-basin ('slow', 'fast', 'stream'). Each water reservoir is represented at the scale
1104 (here: 4 sub-grid units per grid cell), and updated with the lateral in- and outflows at a
1105 daily time-step. The 'slow' water reservoir aggregates the soil drainage, i.e. the vertical
1106 outflow from the 11th layer (2 m depth) of the soil column, effectively representing
1107 'shallow groundwater' transport and storage. The 'fast' water reservoir aggregates
1108 surface runoff simulated in the model, effectively representing overland hydrologic flow.
1109 The 'fast' water reservoir aggregates surface runoff simulated in the model, effectively
1110 representing overland hydrologic flow. The 'slow' and 'fast' water reservoirs feed a
1111 delayed outflow to the 'stream' reservoir' of the next downstream sub-grid quadrant
1112

1113 The water residence time in each reservoir depends on the nature of the reservoir
1114 (increasing residence time in the order: stream < fast < slow reservoir). More generally,
1115 residence time locally decreases with topographic slope and the grid-cell length, used as
1116 a proxy for the main tributary length (Ducharne et al., 2003; Guimberteau et al., 2012).
1117 This is done to reproduce the hydrological effects of geomorphological and topographic
1118 factors in Manning's equation (Manning, 1891) and determines the time that water and
1119 DOC remain in soils prior to entering the river network or groundwater. In this way the
1120 runoff and drainage are exported from sub-unit to sub-unit and from grid-cell to grid-
1121 cell.
1122

1123 2.7 Grid-scale water and carbon routing (Fig. 1f, 1g)

1124 Water-borne, terrestrially-derived DOC and dissolved CO₂ in the soil solution are
1125 exported over the land surface using the same routing scheme. When exported from
1126 soil or litter, DOC remains differentiated in the numerical simulations according to its
1127 initial reactivity within the soil (Active, Slow, Passive). However, because the terrestrial
1128 Slow and Passive DOC pools (Camino-Serrano et al., 2018) are given the same residence
1129 time, these two pools are merged when exported (Lauerwald et al., 2017): Active DOC
1130 flows into a Labile DOC hydrological export pool, while the Slow and Passive DOC pools
1131 flow into a Refractory DOC hydrological pool (Fig. 2b), owing to the fact that the
1132 residence time of these latter soil DOC pools is the same in their original (ORCHIDEE-
1133 SOM) formulation (Camino-Serrano et al., 2018), and retained and merged into a single
1134 hydrological DOC pool in Lauerwald et al. (2017). The water residence times in each
1135 reservoir of each sub-grid scale quadrant determine the decomposition of DOC into CO₂
1136 within water reservoirs, before non-decomposed DOC is passed on to the next reservoir
1137 in the downstream sub-grid quadrant.
1138
1139
1140
1141

Mis en forme	... [66]
Simon Bowring 3/6/y 17:33	
Supprimé: subgrid	
Simon Bowring 3/6/y 17:28	
Mis en forme	... [67]
Simon Bowring 3/6/y 17:33	
Supprimé: subgrid	
Simon Bowring 3/6/y 17:28	
Mis en forme	... [68]
Simon Bowring 3/6/y 10:02	
Supprimé: the	
Simon Bowring 3/6/y 17:28	
Mis en forme	... [69]
Simon Bowring 5/6/y 10:16	
Supprimé: The 'slow' and 'fast' wa	... [70]
Simon Bowring 5/6/y 10:16	
Mis en forme	... [71]
Simon Bowring 3/6/y 17:34	
Supprimé:	
Simon Bowring 3/6/y 17:28	
Mis en forme	... [72]
Simon Bowring 3/6/y 15:21	
Supprimé: the steepness of topography	
Simon Bowring 3/6/y 17:28	
Mis en forme	... [73]
Simon Bowring 3/6/y 15:24	
Supprimé: ,	
Simon Bowring 3/6/y 17:28	
Mis en forme	... [74]
Simon Bowring 3/6/y 15:22	
Supprimé: given by the product of	... [75]
Simon Bowring 3/6/y 17:28	
Mis en forme	... [76]
Unknown	
Code de champ modifié	... [77]
Simon Bowring 3/6/y 15:29	
Supprimé: ,	
Simon Bowring 3/6/y 17:28	
Mis en forme	... [78]
Simon Bowring 3/6/y 15:24	
Supprimé: to	
Simon Bowring 3/6/y 17:28	
Mis en forme	... [79]
Simon Bowring 3/6/y 15:18	
Supprimé: (Ducharne et al., 2003; ... [80]	
Simon Bowring 3/6/y 17:28	
Mis en forme	... [81]
Simon Bowring 5/6/y 10:17	
Supprimé: .	
Simon Bowring 3/6/y 17:28	
Mis en forme	... [82]
Simon Bowring 31/5/y 12:21	
Mis en forme	... [83]
Simon Bowring 5/6/y 10:17	
Mis en forme	... [84]
Simon Bowring 31/5/y 12:21	
Mis en forme	... [85]
Simon Bowring 31/5/y 12:21	
Mis en forme	... [86]
Simon Bowring 5/6/y 10:17	
Supprimé:	
Simon Bowring 3/6/y 17:28	
Mis en forme	... [87]
Unknown	
Code de champ modifié	... [88]
Simon Bowring 3/6/y 17:22	
... [89]	
Simon Bowring 3/6/y 17:28	
Mis en forme	... [90]
Simon Bowring 3/6/y 17:33	
... [91]	
Simon Bowring 3/6/y 17:28	
Mis en forme	... [92]

1196 The river routing calculations, which occur at a daily timestep, are then aggregated to
1197 one-day for the lateral transfer of water, CO_{2(aq)} and DOC from upstream grid to
1198 downstream grid according to the river network. Note that carbonate chemistry in
1199 rivers and total alkalinity routing are not calculated here.

1201 In this framework, the ‘fast’ and ‘slow’ residence times of the water pools in the routing
1202 scheme determine the time that water and DOC remains in overland and groundwater
1203 flow before entering the river network. Note that while we do not explicitly simulate
1204 headwaters, as they exist in a geographically determinant way in the real world, we do
1205 simulate what happens to the water before it flows into a water body large enough to be
1206 represented in the routing scheme by the water pool called ‘stream’, representing a real-
1207 world river of stream order 4 or higher. The ‘fast’ reservoir is thus the runoff water flow
1208 that is destined for entering the ‘stream’ water reservoir, and implicitly represents
1209 headwater streams of Strahler order 1 to 3 by filling the spatial and temporal niche
1210 between overland runoff and the river stem. The dynamics of headwater hydrological
1211 and DOC dynamics (Section 2.10) are of potentially great significance with respect to
1212 carbon processing, as headwater catchments have been shown to be ‘hotspots’ of carbon
1213 metabolism and outgassing in Arctic rivers, despite their relatively small areal
1214 fraction (Denfeld et al., 2013; Drake et al., 2015; Mann et al., 2015; Suzuki et al., 2006;
1215 Venkiteswaran et al., 2014; Vonk et al., 2013, 2015a, 2015b). Thus, in what follows in
1216 this study, we refer to what in the code are called the ‘fast’ and ‘stream’ pools, which
1217 represent the small streams and large stream or river pools, respectively, using ‘stream’
1218 and ‘river’ to denote these from hereon in.

1220 Furthermore, the differentiated representation of water pools as well as mean grid cell
1221 slope, combined with the dynamic active layer simulated for continuous versus
1222 discontinuous permafrost, is important for reproducing the phenomena observed by
1223 Kutscher et al. (2017), and Zhang et al. (2017) for sloping land as shown on the right
1224 hand side of Fig. 1. In discontinuous permafrost and permafrost free regions, these
1225 phenomena encompass landscape processes (sub-grid in the model), through which
1226 water flow is able to re-infiltrate the soil column and so leach more refractory DOC
1227 deeper in the soil column, leading to a more refractory signal in the drainage waters. In
1228 contrast, in continuous permafrost region, the shallow active layer will inhibit the
1229 downward re-infiltration flux of water and encourage leaching at the more organic-rich
1230 and labile surface soil layer, resulting in a more labile DOC signal from the drainage in
1231 these areas (Fig. 1). In addition, places with higher elevation and slope in these regions
1232 tend to experience extreme cold, leading to lower NPP and so DOC leaching. The re-
1233 infiltration processes mentioned are thought to be accentuated in areas with higher
1234 topographic relief (Jasechko et al., 2016), which is why they are represented on sloping
1235 areas in Fig. 1.

1236 **2.8 Representation of floodplain hydrology and their DOC budget (Fig. 1e,1h)**

1239 The third terrestrial DOC export pathway in MICT-L is through flooding of floodplains, a
1240 transient period that occurs when stream water is forced by high discharge rates over
1241 the river ‘banks’ and flows onto a flat floodplain area of the grid cell that the river
1242 crosses, thus inundating the soil. Such a floodplain area is represented as a fraction of a
1243 grid-cell with the maximum extent of inundation, termed the ‘potential flooded area’
1244 being predefined from a forcing file (Tootchi et al., 2019). Here, the DOC pools that are

Simon Bowring 31/5/y 12:48
Supprimé: streams

Simon Bowring 31/5/y 12:21
Mis en forme: Anglais (G.B.)

Simon Bowring 31/5/y 12:48
Supprimé: river

Simon Bowring 31/5/y 12:21
Mis en forme: Anglais (G.B.)

Simon Bowring 5/6/y 10:41
Mis en forme: Police :Non Italique

Simon Bowring 31/5/y 12:21
Mis en forme: Anglais (G.B.)

Simon Bowring 31/5/y 12:49
Supprimé: , which is indicative of the pool of

Simon Bowring 31/5/y 12:21
Mis en forme: Vérifier l'orthographe et la grammaire

Simon Bowring 31/5/y 12:21
Mis en forme: Vérifier l'orthographe et la grammaire

Simon Bowring 31/5/y 12:21
Mis en forme ... [93]

Simon Bowring 31/5/y 12:50
Supprimé: is

Simon Bowring 3/6/y 15:46
Mis en forme: Police :Non Italique

Simon Bowring 3/6/y 15:46
Supprimé: implicitly representativ ... [94]

Simon Bowring 31/5/y 12:21
Mis en forme ... [95]

Simon Bowring 31/5/y 12:21
Mis en forme ... [96]

Simon Bowring 31/5/y 12:21
Mis en forme ... [97]

Simon Bowring 31/5/y 12:21
Mis en forme ... [98]

Simon Bowring 31/5/y 12:21
Mis en forme ... [99]

Simon Bowring 31/5/y 12:21
Mis en forme ... [100]

Simon Bowring 31/5/y 12:21
Mis en forme: Anglais (G.B.)

Simon Bowring 31/5/y 13:44
Supprimé: These

Unknown
Code de champ modifié

Simon Bowring 31/5/y 12:21
Mis en forme ... [101]

Simon Bowring 31/5/y 12:21
Mis en forme ... [102]

Simon Bowring 31/5/y 12:21
Mis en forme ... [103]

1258 already being produced in these inundated areas from litter and SOC decomposition in
1259 the first 5 layers of the soil column are directly absorbed by the overlying flood waters.
1260 These flood waters may then either process the DOC directly, via oxidation to CO₂,
1261 (Sections 2.10, 2.11) or return them to the river network, as floodwaters recede to the
1262 river main stem, at which point they join the runoff and drainage export flows from
1263 upstream.

1264 MICT-L includes the floodplain hydrology part of the routing scheme (D'Orgeval et al.,
1265 2008; Guimberteau et al., 2012), as well as additions and improvements described in
1266 Lauerwald et al. (2017). The spatial areas that are available for potential flooding are
1267 pre-defined by an input map originally based on the map of Prigent et al. (2007).
1268 However, for this study, we used an alternative map of the "regularly flooded areas"
1269 derived from the method described in Tootchi et al. (2019), which in this study uses an
1270 improved input potential flooding area forcing file specific to the Lena basin, that
1271 combines three high-resolution surface water and inundation datasets derived from
1272 satellite imagery: GIEMS-D15 (Fluet-Chouinard et al., 2015), which results from the
1273 downscaling of the map of Prigent et al. (2007) at 15-arc-sec (ca 500 m at Equator);
1274 ESA-CCI land cover (at 300 m ~ 10 arc-sec); and JRC surface water at 1 arc-sec (Pekel
1275 et al., 2016). The 'fusion' approach followed by this forcing dataset stems from the
1276 assumption that the potential flooding areas identified by the different datasets are all
1277 valid despite their uncertainties, although none of them is exhaustive. The resulting map
1278 was constructed globally at the 15 arc-sec resolution and care was taken to exclude
1279 large permanent lakes from the potential flooding area based on the HydroLAKES
1280 database (Messenger et al., 2016). In the Lena river basin, the basin against which we
1281 evaluate ORCHIDEE MICT-LEAK in Part 2 of this study, this new potential floodplains file
1282 gives a maximum floodable area of 12.1% (2.4*10⁵ km²) of the 2.5*10⁶ km² basin,
1283 substantially higher than previous estimates of 4.2% by Prigent et al. (2007).

1286 With this improved forcing, river discharge becomes available to flood a specific pre-
1287 defined floodplain grid fraction, creating a temporary floodplains hydrologic reservoir,
1288 whose magnitude is defined by the excess of discharge at that point over a threshold
1289 value, given by the median simulated water storage of water in each grid cell over a 30
1290 year period. The maximum extent of within-grid flooding is given by another threshold,
1291 the calculated height of flood waters beyond which it is assumed that the entire grid is
1292 inundated. This height, which used to be fixed at 2 m, is now determined by the 90th
1293 percentile of all flood water height levels calculated per grid cell from total water
1294 storage of that grid cell over a reference simulation period for the Lena basin, using the
1295 same methodology introduced by Lauerwald et al. (2017). The residence time of water
1296 on the floodplains (τ_{flood}) is a determinant of its resulting DOC concentration, since
1297 during this period it appropriates all DOC produced by the top 5 layers of the soil
1298 column.

1300 2.9 Oceanic outflow (Fig. 1i)

1302 Routing of water and DOC through the river network ultimately lead to their export
1303 from the terrestrial system at the river mouth (Fig. 1), which for high latitude rivers are
1304 almost entirely sub-deltas of the greater 'estuary', described by McClelland et al. (2012),
1305 draining into the Arctic Ocean. Otherwise, the only other loss pathway for carbon
1306 export once in the river network is through its decomposition to CO₂ and subsequent

Simon Bowring 31/5/y 12:21
Mis en forme: Vérifier l'orthographe et la grammaire

Simon Bowring 31/5/y 12:21
Mis en forme: Vérifier l'orthographe et la grammaire

Simon Bowring 31/5/y 12:21
Mis en forme: Vérifier l'orthographe et la grammaire

Simon Bowring 31/5/y 12:21
Mis en forme: Vérifier l'orthographe et la grammaire

Simon Bowring 30/5/y 14:43
Supprimé: 9

Simon Bowring 31/5/y 12:21
Mis en forme: Vérifier l'orthographe et la grammaire

Simon Bowring 31/5/y 12:21
Mis en forme: Vérifier l'orthographe et la grammaire

Simon Bowring 31/5/y 12:21
Mis en forme: Vérifier l'orthographe et la grammaire

Simon Bowring 31/5/y 12:21
Mis en forme: Vérifier l'orthographe et la grammaire

Simon Bowring 31/5/y 12:21
Mis en forme: Vérifier l'orthographe et la grammaire

Simon Bowring 31/5/y 12:21
Mis en forme: Vérifier l'orthographe et la grammaire

Simon Bowring 31/5/y 12:21
Mis en forme: Anglais (G.B.)

Simon Bowring 31/5/y 12:21
Mis en forme: Vérifier l'orthographe et la grammaire

Simon Bowring 31/5/y 12:21
Mis en forme: Vérifier l'orthographe et la grammaire

Simon Bowring 31/5/y 12:21
Mis en forme: Anglais (G.B.)

Simon Bowring 31/5/y 12:21
Mis en forme: ... [104]

1308 escape to the atmosphere from the river surface. DOC decomposition is ascribed a
 1309 constant fraction for the labile and refractory DOC pools of 0.3 d⁻¹ and 0.01 d⁻¹ at 25°C,
 1310 respectively, these modulated by a water-temperature dependent Arrhenius rate term.
 1311 Because the concentration of dissolved CO₂ (referred to as CO_{2(aq)}) in river water is
 1312 derived not only from in-stream decomposition of DOC, but also from CO_{2(aq)} inputs
 1313 from the decomposition of litter, SOC and DOC both in upland soils and in inundated
 1314 soils, the model also represents the lateral transport of CO_{2(aq)} from soils through the
 1315 river network. Note that autochthonous primary production and derivative carbon
 1316 transformations are ignored here, as they are considered relatively minor contributors
 1317 in the Arctic lateral flux system (Cauwet and Sidorov, 1996; Sorokin and Sorokin, 1996).

1319 2.10 Dissolved CO₂ export and river evasion (Fig. 1j)

1321 Soil CO_{2(aq)} exports are simulated by first assuming a constant concentration of CO_{2(aq)}
 1322 with surface runoff and drainage water fluxes, of 20 and 2 mgC L⁻¹, corresponding to a
 1323 pCO₂ of 50000 μ atm and 5000 μ atm at 25°C in the soil column, respectively. These
 1324 quantities are then scaled with total (root, microbial, litter) soil respiration by a scaling
 1325 factor first employed in Lauerwald et al. (2019, *in review*). In the high latitudes soil
 1326 respiration is dominantly controlled by microbial decomposition, and for the Lena basin
 1327 initial model tests suggest that its proportional contribution to total respiration is
 1328 roughly 90%, versus 10% from root respiration. Thus CO_{2(aq)} enters and circulates the
 1329 rivers via the same routing scheme as that for DOC and river water. The lateral transfers
 1330 of carbon are aggregated from the 30 minute time steps at which they are calculated,
 1331 with a 48 timestep period, so that they occur within the model as a daily flux. The
 1332 calculation of the river network pCO₂ can then be made from CO_{2(aq)} and its equilibrium
 1333 with the atmosphere, which is a function of its solubility (K_{CO2}) with respect to the
 1334 temperature of the water surface T_{WATER} (Eq.2).

$$(2) \text{ pCO}_{2\text{POOL}} = \frac{[\text{CO}_{2(aq)}]}{12.011 * K_{\text{CO}_2}}$$

1336 Where the pCO₂ (atm.) of a given (e.g. 'stream', 'fast', 'slow' and floodplain) water pool
 1337 (pCO_{2POOL}) is given by the dissolved CO₂ concentration in that pool [CO_{2(aq)}], the molar
 1338 weight of carbon (12.011 g mol⁻¹) and K_{CO2}. Water temperature (T_{WATER}, (°C)) isn't
 1339 simulated by the model, but is derived here from the average daily surface temperature
 1340 (T_{GROUND}, (°C)) in the model (Eq. 3), a derivation calculated for ORCHIDEE by Lauerwald
 1341 et al. (2017) and retained here. Note that while dissolved CO₂ enters from the terrestrial
 1342 reservoir from organic matter decomposition, it is also generated *in situ* within the river
 1343 network as DOC is respired microbially.

1346 With our water temperature estimate, both K_{CO2} and the Schmidt number (Sc, Eq. 4)
 1347 from Wanninkhof (1992) can be calculated, allowing for simulation of actual gas
 1348 exchange velocities from standard conditions. The Schmidt number links the gas
 1349 transfer velocity of any soluble gas (in this case carbon dioxide) from the water surface
 1350 to water temperature. For more on the Schmidt number see (Wanninkhof, 2014, 1992).
 1351 The CO₂ that evades is then subtracted from the [CO_{2(aq)}] stocks of each of the different
 1352 hydrologic reservoirs –river, flood and stream.

$$(3) T_{\text{WATER}} = 6.13^{\circ}\text{C} + (0.8 * T_{\text{GROUND}})$$

Simon Bowring 31/5/y 12:21
 Mis en forme: Vérifier l'orthographe et la grammaire

Unknown
 Code de champ modifié

Simon Bowring 31/5/y 12:21
 Mis en forme ... [105]

Simon Bowring 31/5/y 13:46
 Supprimé: ...scaling factor first e... [106]

Simon Bowring 31/5/y 12:21
 Mis en forme ... [107]

Simon Bowring 31/5/y 12:21
 Mis en forme ... [108]

Simon Bowring 5/6/y 10:31
 Mis en forme: Police :Non Italique

Simon Bowring 5/6/y 10:31
 Mis en forme: Police :Non Italique

Simon Bowring 5/6/y 10:30
 Supprimé: Where the pCO₂ of a given (e.g. 'stream', 'fast', 'slow' and floodplain) water pool (pCO_{2POOL}) is given by [CO_{2(aq)}] the dissolved CO₂ concentration in that pool, and K_{CO2}.

Simon Bowring 31/5/y 12:21
 Mis en forme ... [109]

Simon Bowring 31/5/y 14:48
 Supprimé: a set up used

Simon Bowring 31/5/y 12:21
 Mis en forme: Vérifier l'orthographe et la grammaire

Simon Bowring 31/5/y 12:21
 Mis en forme ... [110]

Simon Bowring 31/5/y 12:21
 Mis en forme ... [111]

Simon Bowring 30/5/y 16:38
 Supprimé: [CO₂]

Simon Bowring 31/5/y 12:21
 Mis en forme ... [112]

1371

$$(4) Sc = ((1911 - 118.11) * T_{WATER}) + (3.453 * T_{WATER}^2) - (0.0413 * T_{WATER}^3)$$

1372

1373 CO₂ evasion is therefore assumed to originate from the interplay of CO₂ solubility,
 1374 relative gradient in partial pressures of CO₂ between air and water, and gas exchange
 1375 kinetics. Evasion as a flux from river and floodplain water surfaces is calculated at a
 1376 daily timestep, however in order to satisfy the sensitivity of the relative gradient of
 1377 partial pressures of CO₂ in the water column and atmosphere to both CO₂ inputs and
 1378 evasion, the pCO₂ of water is calculated at a more refined 6 minute timestep. The daily
 1379 lateral flux of CO₂ inputs to the water column are thus equally broken up into 240 (6
 1380 min.) segments per day and distributed to the pCO₂ calculation. Other relevant carbon
 1381 processing pathways, such as the photochemical breakdown of riverine [dissolved](#)
 1382 [organic carbon](#), are not explicitly included here, despite the suggestion by some studies
 1383 that the photochemical pathway dominate DOC processing in Arctic streams (e.g. Cory et
 1384 al., 2014). Rather, these processes are bundled into the aggregate decomposition rates
 1385 used in the model, which thus include both microbial and photochemical oxidation. This
 1386 is largely because it is unclear how different factors contribute to breaking down DOC in
 1387 a dynamic environment and also the extent to which our DOC decomposition and CO₂
 1388 calculations implicitly include both pathways –e.g. to what extent the equations and
 1389 concepts used in their calculation confound bacterial with photochemical causation,
 1390 since both microbial activity and incident UV light are a function of temperature and
 1391 total incident light.

1392

1393 2.11 Soil layer processes: turbation (Fig. 1k), adsorption (Fig. 1l)

1394

1395 The soil carbon module is discretised into a 32-layer scheme totalling 38m depth, which
 1396 it shares with the soil thermodynamics to calculate temperature through the entire
 1397 column. An aboveground snow module (Wang et al., 2013) is discretised into 3 layers of
 1398 differing thickness, heat conductance and density, which collectively act as a
 1399 thermodynamically-insulating intermediary between soil and atmosphere (Fig. 2a).
 1400 Inputs to the three soil carbon pools are resolved only for the top 2m of the soil, where
 1401 litter and DOC are exchanged with SOC in decomposition and adsorption/desorption
 1402 processes. Decomposition of SOC pools, calculated in each soil layer, is dependent on
 1403 soil temperature, moisture and texture (Koven et al., 2009; Zhu et al., 2016), while
 1404 vertical transfer of SOC is enabled by representation of cryoturbation (downward
 1405 movement of matter due to repeated freeze-thaw) in permafrost regions, and
 1406 bioturbation (by soil organisms) in non-permafrost regions in terms of a diffusive flux.

1407

1408 Cryoturbation, given a diffusive mixing rate (Diff) of 0.001 m² yr⁻¹ (Koven et al., 2009),
 1409 is possible to 3 m depth (diffusive rate declines linearly to zero from active layer bottom to
 1410 3 m), and extends the soil column carbon concentration depth in permafrost regions
 1411 from 2 m. Bioturbation is possible to 2 m depth, with a mixing rate of 0.0001 m² yr⁻¹
 1412 (Koven et al., 2013) declining to zero at 2 m (Eq. 5). In MICT-L, these vertical exchanges
 1413 in the soil column are improved on. Now, we explicitly include the cryoturbation and
 1414 bioturbation of both belowground litter and DOC. These were not possible in
 1415 ORCHIDEE-MICT because, for the former, the belowground litter distribution was not
 1416 explicitly discretised or vertically dynamic, and for the latter because DOC was not
 1417 produced in prior versions. Diffusion is given by :

1418

Simon Bowring 31/5/y 12:21

Mis en forme

... [113]

Simon Bowring 30/5/y 16:36

Supprimé: OC

Simon Bowring 31/5/y 12:21

Mis en forme

... [114]

Simon Bowring 31/5/y 12:21

Mis en forme

... [115]

Simon Bowring 31/5/y 12:21

Mis en forme

... [116]

Simon Bowring 31/5/y 12:33

Supprimé: of

Simon Bowring 31/5/y 12:21

Mis en forme

... [117]

$$(5) \quad \frac{\delta DOC_i(z)}{\delta t} = IN_{DOC_i}(z) - k_i(z) * \phi * DOC_i(z) + Diff \frac{\delta DOC_i^2(z)}{\delta z^2}$$

Where DOC_i is the DOC in pool i at depth z , ($gC\ m^{-3}$) IN_{DOC_i} the inflow of carbon to that pool ($gCm^{-3}d^{-1}$), k_i the decomposition rate of that pool (d^{-1}), Φ the temperature dependent rate modifier for DOC decomposition and $Diff$ the diffusion coefficient ($m^2\ yr^{-1}$). The vertical diffusion of DOC in non-permafrost soils represented here (that is, the non-cryoturbated component) appears to be consistent with recent studies reporting an increased retention of DOC in the deepening active layer of organic soils (Zhang et al., 2017). This vertical translocation of organic carbon, whether in solid/liquid phase appears to be an important component of the high rates of SOC buildup observed at depth in deep permafrost soils.

2.11 Priming (Fig. 1m)

MICT-L also incorporates a scheme for the 'priming' of organic matter decomposition, a process in which the relative stability of SOC is impacted by the intrusion of or contact with SOC of greater reactivity, resulting in enhanced rates of decomposition. This was first introduced by Guenet et al. (2016), and updated in Guenet et al. (2018). This process has shown itself to be of potentially large significance for SOC stocks and their respiration in high latitude regions, in empirical in situ and soil incubation studies (De Baets et al., 2016; Walz et al., 2017; Wild et al., 2014, 2016; Zhang et al., 2017), as well as modelling exercises (Guenet et al., 2018). Here, priming of a given soil pool is represented through the decomposition of soil carbon ($dSOC/dt$) by the following equation :

$$(6) \quad \frac{dSOC}{dt} = IN_{SOC} - k * (1 - e^{-c*FOC}) * SOC * \theta * \phi * \gamma$$

Where IN_{SOC} is the carbon input to that pool, k is the SOC decomposition rate ($1/dt$), FOC (Kg) is a stock of matter interacting with this SOC pool to produce priming, c is a parameter controlling this interaction, SOC is the SOC reservoir (Kg), and θ , Φ and γ the zero-dimensional moisture, temperature and soil texture rate modifiers that modulate decomposition in the code, and are originally determined by the CENTURY formulation (Parton et al., 1987) and subsequently re-estimated to include priming in Guenet et al., (2016, 2018)."

The variable FOC ('fresh organic carbon') is an umbrella term used for specifying all of the carbon pools which together constitute that carbon which is considered potential priming donor material -ie. more labile - to a given receptor carbon pool. Thus, for the slow soil carbon pool FOC incorporates the active soil carbon pool plus the above and below ground structural and metabolic litter pools, because these pools are donors to the slow pool, and considered to accelerate its turnover through priming. Importantly, previous studies with priming in ORCHIDEE employed this scheme on a version which resolves neither the vertical discretisation of the soil column nor the explicit vertical diffusion processes presented here. This is potentially significant, since the vertical diffusion of relatively reactive matter may strongly impact (accelerate) the decomposition of low reactivity matter in the deeper non-frozen horizons of high latitude soils, while the explicit discretisation of the soil column is a significant improvement in terms of the accuracy of process-representation within the column

Simon Bowring 31/5/y 12:21

Mis en forme

... [118]

Simon Bowring 31/5/y 12:21

Mis en forme

... [119]

Simon Bowring 31/5/y 12:21

Mis en forme

... [120]

Simon Bowring 31/5/y 12:21

Mis en forme

... [121]

Simon Bowring 31/5/y 12:21

Mis en forme

... [122]

Simon Bowring 5/6/y 10:25

Supprimé: fonctions

Simon Bowring 31/5/y 12:21

Mis en forme: Vérifier l'orthographe et la grammaire

Simon Bowring 31/5/y 15:01

Supprimé: e

Simon Bowring 31/5/y 12:21

Mis en forme

... [123]

Simon Bowring 31/5/y 12:33

Supprimé: u

1474 itself.

1475
1476 Other carbon-relevant schemes included in MICT-L are: A prognostic fire routine
1477 (SPITFIRE), calibrated for the trunk version of ORCHIDEE (Yue et al., 2016) is available
1478 in our code but not activated in the simulations conducted here. As a result, we do not
1479 simulate the ~13% of Arctic riverine DOC attributed to biomass burning by Myers-Pigg
1480 et al. (2015), or the ~8% of DOC discharge to the Arctic Ocean from the same source
1481 (Stubbins et al., 2017). Likewise, a crop harvest module consistent with that in
1482 ORCHIDEE-MICT exists in MICT-L but remains deactivated for our simulations.

1483
1484 A module introduced in the last version of ORCHIDEE-MICT (Guimberteau et al., 2018),
1485 in which the soil thermal transfer and porosity and moisture are strongly affected by
1486 SOC concentration, is deactivated here, because it is inconsistent with the new DOC
1487 scheme. Specifically, while carbon is conserved in both MICT and MICT-L soil schemes,
1488 MICT-L introduces a new reservoir into which part of the total organic carbon in the soil
1489 –the DOC –must now go. This then lowers the SOC concentration being read by this
1490 thermix module, causing significant model artefact in soil thermodynamics and
1491 hydrology in early exploratory simulations. Ensuring compatibility of this routine with
1492 the DOC scheme will be a focal point of future developments in MICT-L. Other processes
1493 being developed for ORCHIDEE-MICT, including a high latitude peat formation (Qiu et
1494 al., 2018), methane production and microbial heat generating processes that are being
1495 optimised and calibrated, are further pending additions to this particular branch of the
1496 ORCHIDEE-MICT series.

1497 3 Soil Carbon Spinup and Simulation Protocol

1500 The soil carbon spinup component of ORCHIDEE, which is available to both its trunk and
1501 MICT branches, was omitted from this first version of MICT-L, owing to the code burden
1502 required for ensuring compatibility with the soil carbon scheme in MICT-L. However,
1503 because we are simulating high latitude permafrost regions, having a realistic soil
1504 carbon pool at the outset of the simulations is necessary if we are to untangle the
1505 dynamics of SOC and DOC with a changing environment. Because the soil carbon spinup
1506 in ORCHIDEE-MICT is normally run over more than 10,000 years (Guimberteau et al.,
1507 2108), and because running MICT-L for this simulation period in its normal, non-spinup
1508 simulation mode would impose an unreasonable burden on computing resources, here
1509 we directly force the soil carbon output from a MICT spinup directly into the restart file
1510 of a MICT-L simulation.

1512 A 20,000 year spinup loop over 1961-1990 (these years chosen to mimic coarsely
1513 warmer mid-Holocene climate) -forced by GSWP-3 climatology, whose configuration
1514 derives directly from that used in Guimberteau et al. (2018), was thus used to replace
1515 the three soil carbon pool values from a 1-year MICT-L simulation to set their initial
1516 values. A conversion of this soil carbon from volumetric to areal units was applied,
1517 owing to different read/write standards in ORCHILEAK versus ORCHIDEE-MICT. This
1518 artificially imposed, MICT-derived SOC stock would then have to be exposed to MICT-L
1519 code, whose large differences in soil carbon module architecture as compared to MICT,
1520 would drive a search for new equilibrium soil carbon stocks.

1522 Due to the long residence times of the passive SOC pool, reaching full equilibrium for it

Simon Bowring 31/5/y 12:21
Mis en forme: Vérifier l'orthographe et la grammaire

Simon Bowring 31/5/y 12:21
Mis en forme: Vérifier l'orthographe et la grammaire

Simon Bowring 31/5/y 12:21
Mis en forme: Vérifier l'orthographe et la grammaire

Simon Bowring 31/5/y 12:21
Mis en forme: Vérifier l'orthographe et la grammaire

Simon Bowring 31/5/y 12:21
Mis en forme: Vérifier l'orthographe et la grammaire

Simon Bowring 31/5/y 12:21
Mis en forme: Vérifier l'orthographe et la grammaire

Simon Bowring 31/5/y 12:21
Mis en forme: Vérifier l'orthographe et la grammaire

Simon Bowring 31/5/y 12:21
Mis en forme: Vérifier l'orthographe et la grammaire

Simon Bowring 31/5/y 12:21
Mis en forme: Vérifier l'orthographe et la grammaire

Simon Bowring 31/5/y 12:21
Mis en forme: Vérifier l'orthographe et la grammaire

Simon Bowring 31/5/y 12:21
Mis en forme: Vérifier l'orthographe et la grammaire

1523 requires a simulation length on the order of 20,000y –again an overburden. As we are
1524 interested primarily in DOC in this study, which derives mostly from the Active and Slow
1525 SOC pools, the model was run until these two pools reached a quasi-steady state
1526 equilibria (Part 2 Supplement, Fig. S1). This was done by looping over the same 30 year
1527 cycle (1901-1930) of climate forcing data from GSWP-3 during the pre-industrial period
1528 (Table 1) and the first year (1901) of a prescribed vegetation map (ESA CCI Land Cover
1529 Map, Bontemps et al., (2013)) –to ensure equilibrium of DOC, dissolved CO₂ and Active
1530 and Slow SOC pools is driven not just by a single set of environmental factors in one year
1531 –for a total of 400 years. The parameter configuration adhered as close as possible to
1532 that used in the original ORCHIDEE-MICT spinup simulations, to avoid excessive
1533 equilibrium drift from the original SOC state (Fig. 3).
1534

1535 4 Conclusion

1536 This first part of a two-part study has described a new branch of the high latitude
1537 version of ORCHIDEE-MICT land surface model, in which the production, transport and
1538 transformation of DOC and dissolved CO₂ in soils and along the inland water network of
1539 explicitly-represented northern permafrost regions has been implemented for the first
1540 time. Novel processes with respect to ORCHIDEE-MICT include the discretisation of
1541 litter inputs to the soil column, the production of DOC and CO_{2(aq.)} from organic matter
1542 and decomposition, respectively, transport of DOC into the river routing network and its
1543 potential mineralisation to CO_{2(aq.)} in the water column, as well as subsequent evasion
1544 from the water surface to the atmosphere. In addition, an improved floodplains
1545 representation has been implemented which allows for the hydrologic cycling of DOC
1546 and CO₂ in these inundated areas. In addition to descriptions of these processes, this
1547 paper outlines the protocols and configuration adopted for simulations using this new
1548 model that will be used for its evaluation over the Lena river basin in the second part of
1549 this study.
1550

1551 Code and data availability

1552 The source code for ORCHIDEE MICT-LEAK revision 5459 is available via
1553 [http://forge.ipsl.jussieu.fr/orchidee/wiki/GroupActivities/CodeAvailabilityPublication/
1554 ORCHIDEE_gmd-2018-MICT-LEAK_r5459](http://forge.ipsl.jussieu.fr/orchidee/wiki/GroupActivities/CodeAvailabilityPublication/ORCHIDEE_gmd-2018-MICT-LEAK_r5459)
1555

1556 Primary data and scripts used in the analysis and other supplementary information that
1557 may be useful in reproducing the author's work can be obtained by contacting the
1558 corresponding author.
1559

1560 This software is governed by the CeCILL license under French law and abiding by the
1561 rules of distribution of free software. You can use, modify and/or redistribute the
1562 software under the terms of the CeCILL license as circulated by CEA, CNRS and INRIA at
1563 the following URL: <http://www.cecill.info>.
1564

1565 Authors' contribution

1566 SB coded this model version, conducted the simulations and wrote the main body of the
1567 paper. RL gave consistent input to the coding process and made numerous code
1568 improvements and bug fixes. BG advised on the inclusion of priming processes in the
1569 model and advised on the study design and model configuration; DZ gave input on the
1570 modelled soil carbon processes and model configuration. MG, AT and AD contributed to
1571

Simon Bowring 4/6/y 09:19

Supprimé:

Simon Bowring 31/5/y 12:21

Mis en forme: Vérifier l'orthographe et la grammaire

Simon Bowring 4/6/y 09:18

Supprimé:

Simon Bowring 31/5/y 12:21

Mis en forme: Vérifier l'orthographe et la grammaire

Simon Bowring 31/5/y 12:21

Mis en forme: Vérifier l'orthographe et la grammaire

Simon Bowring 31/5/y 12:21

Mis en forme: Vérifier l'orthographe et la grammaire

Simon Bowring 4/6/y 09:19

Supprimé:

Simon Bowring 31/5/y 12:21

Mis en forme: Vérifier l'orthographe et la grammaire

Simon Bowring 31/5/y 12:21

Mis en forme: Anglais (G.B.)

Simon Bowring 31/5/y 12:21

Mis en forme: Police par défaut, Anglais (G.B.)

Simon Bowring 31/5/y 12:21

Mis en forme: Anglais (G.B.)

1575 improvements in hydrological representation and floodplain forcing data. PC oversaw
1576 all developments leading to the publication of this study. All authors contributed to
1577 suggestions regarding the final content of the study.

1578

1579 **Competing interests**

1580 The authors declare no competing financial interests.

1581

1582 **Acknowledgements**

1583 Simon Bowring acknowledges funding from the European Union's Horizon 2020
1584 research and innovation program under the Marie Skłodowska-Curie grant agreement
1585 No. 643052, 'C-CASCADES' program. Simon Bowring received a PhD grant. Matthieu
1586 Guimberteau acknowledges funding from the European Research Council Synergy grant
1587 ERC-2013-SyG-610028 IMBALANCE-P. Ronny Lauerwald acknowledges funding from
1588 the European Union's Horizon 2020 research and innovation program under grant
1589 agreement no.703813 for the Marie Skłodowska-Curie European Individual Fellowship
1590 "C-Leak".

1591

1592 **References:**

1593

1594 Aitkenhead-Peterson, J. A., McDowell, W. H. and Neff, J. C.: Sources, Production, and
1595 Regulation of Allochthonous Dissolved Organic Matter Inputs to Surface Waters, in
1596 Aquatic Ecosystems., 2003.

1597 De Baets, S., Van de Weg, M. J., Lewis, R., Steinberg, N., Meersmans, J., Quine, T. A., Shaver,
1598 G. R. and Hartley, I. P.: Investigating the controls on soil organic matter decomposition in
1599 tussock tundra soil and permafrost after fire, *Soil Biol. Biochem.*,
1600 doi:10.1016/j.soilbio.2016.04.020, 2016.

1601 Bardy, M., Derenne, S., Allard, T., Benedetti, M. F. and Fritsch, E.: Podzolisation and
1602 exportation of organic matter in black waters of the Rio Negro (upper Amazon basin,
1603 Brazil), *Biogeochemistry*, doi:10.1007/s10533-010-9564-9, 2011.

1604 Bauch, D., Hölemann, J. A., Nikulina, A., Wegner, C., Janout, M. A., Timokhov, L. A. and
1605 Kassens, H.: Correlation of river water and local sea-ice melting on the Laptev Sea shelf
1606 (Siberian Arctic), *J. Geophys. Res. Ocean.*, doi:10.1002/jgrc.20076, 2013.

1607 Berezovskaya, S., Yang, D. and Hinzman, L.: Long-term annual water balance analysis of
1608 the Lena River, *Glob. Planet. Change*, doi:10.1016/j.gloplacha.2004.12.006, 2005.

1609 Bergkvist, B. O. and Folkesson, L.: Soil acidification and element fluxes of a *Fagus sylvatica*
1610 forest as influenced by simulated nitrogen deposition, *Water, Air, Soil Pollut.*,
1611 doi:10.1007/BF00482753, 1992.

1612 Bogard, M. J., Kuhn, C. D., Johnston, S. E., Striegl, R. G., Holtgrieve, G. W., Dornblaser, M. M.,
1613 Spencer, R. G. M., Wickland, K. P. and Butman, D. E.: Negligible cycling of terrestrial
1614 carbon in many lakes of the arid circumpolar landscape, *Nat. Geosci.*,
1615 doi:10.1038/s41561-019-0299-5, 2019.

1616 Bontemps, S., Defourny, P., Radoux, J., Van Bogaert, E., Lamarche, C., Achard, F., Mayaux,
1617 P., Boettcher, M., Brockmann, C., Kirches, G., Zülkhe, M., Kalogirou, V., Seifert, F. . and
1618 Arino, O.: Consistent global land cover maps for climate modelling communities: current
1619 achievements of the ESA' and cover CCI, in *ESA Living Planet Symposium 2013.*, 2013.

1620 Camino-Serrano, M., Gielen, B., Luyssaert, S., Ciais, P., Vicca, S., Guenet, B., Vos, B. De,
1621 Cools, N., Ahrens, B., Altaf Arain, M., Borcken, W., Clarke, N., Clarkson, B., Cummins, T.,
1622 Don, A., Pannatier, E. G., Laudon, H., Moore, T., Nieminen, T. M., Nilsson, M. B., Peichl, M.,
1623 Schwendenmann, L., Siemens, J. and Janssens, I.: Linking variability in soil solution

Simon Bowring 31/5/y 12:21

Mis en forme: Anglais (G.B.)

Simon Bowring 31/5/y 12:21

Mis en forme: Vérifier l'orthographe et la grammaire

Simon Bowring 31/5/y 12:21

Mis en forme: Vérifier l'orthographe et la grammaire

1624 dissolved organic carbon to climate, soil type, and vegetation type, *Global Biogeochem.*
1625 *Cycles*, doi:10.1002/2013GB004726, 2014.
1626 Camino-Serrano, M., Guenet, B., Luysaert, S., Ciais, P., Bastrikov, V., De Vos, B., Gielen, B.,
1627 Gleixner, G., Jornet-Puig, A., Kaiser, K., Kothawala, D., Lauerwald, R., Peñuelas, J.,
1628 Schrumpf, M., Vicca, S., Vuichard, N., Walmsley, D. and Janssens, I. A.: ORCHIDEE-SOM:
1629 Modeling soil organic carbon (SOC) and dissolved organic carbon (DOC) dynamics along
1630 vertical soil profiles in Europe, *Geosci. Model Dev.*, doi:10.5194/gmd-11-937-2018,
1631 2018.
1632 Cauwet, G. and Sidorov, I.: The biogeochemistry of Lena River: Organic carbon and
1633 nutrients distribution, in *Marine Chemistry.*, 1996.
1634 Clarke, N., Wu, Y. and Strand, L. T.: Dissolved organic carbon concentrations in four
1635 Norway spruce stands of different ages, *Plant Soil*, doi:10.1007/s11104-007-9384-4,
1636 2007.
1637 Cory, R. M., Ward, C. P., Crump, B. C. and Kling, G. W.: Sunlight controls water column
1638 processing of carbon in arctic fresh waters, *Science (80-.)*,
1639 doi:10.1126/science.1253119, 2014.
1640 D'Orgeval, T., Polcher, J. and De Rosnay, P.: Sensitivity of the West African hydrological
1641 cycle in ORCHIDEE to infiltration processes, *Hydrol. Earth Syst. Sci.*, doi:10.5194/hess-
1642 12-1387-2008, 2008.
1643 DeLuca, T. H. and Boisvenue, C.: Boreal forest soil carbon: Distribution, function and
1644 modelling, *Forestry*, doi:10.1093/forestry/cps003, 2012.
1645 Denfeld, B., Frey, K. and Sobczak, W.: Summer CO₂ evasion from streams and rivers in
1646 the Kolyma River basin, north-east Siberia, *Polar ...*, doi:10.3402/polar.v32i0.19704,
1647 2013.
1648 Dery, S. J., Stadnyk, T. A., MacDonald, M. K. and Gauli-Sharma, B.: Recent trends and
1649 variability in river discharge across northern Canada, *Hydrol. Earth Syst. Sci.*,
1650 doi:10.5194/hess-20-4801-2016, 2016.
1651 Drake, T. W., Wickland, K. P., Spencer, R. G. M., McKnight, D. M. and Striegl, R. G.: Ancient
1652 low-molecular-weight organic acids in permafrost fuel rapid carbon dioxide production
1653 upon thaw, *Proc. Natl. Acad. Sci.*, doi:10.1073/pnas.1511705112, 2015.
1654 Ducharne, A., Golaz, C., Leblois, E., Laval, K., Polcher, J., Ledoux, E. and De Marsily, G.:
1655 Development of a high resolution runoff routing model, calibration and application to
1656 assess runoff from the LMD GCM, *J. Hydrol.*, doi:10.1016/S0022-1694(03)00230-0,
1657 2003.
1658 Findlay, H. S., Gibson, G., Kędra, M., Morata, N., Orchowska, M., Pavlov, A. K., Reigstad, M.,
1659 Silyakova, A., Tremblay, J.-É., Walczowski, W., Weydmann, A. and Logvinova, C.:
1660 Responses in Arctic marine carbon cycle processes: conceptual scenarios and
1661 implications for ecosystem function, *Polar Res.*, doi:10.3402/polar.v34.24252, 2015.
1662 Fluet-Chouinard, E., Lehner, B., Rebelo, L. M., Papa, F. and Hamilton, S. K.: Development
1663 of a global inundation map at high spatial resolution from topographic downscaling of
1664 coarse-scale remote sensing data, *Remote Sens. Environ.*, doi:10.1016/j.rse.2014.10.015,
1665 2015.
1666 Frey, K. E. and McClelland, J. W.: Impacts of permafrost degradation on arctic river
1667 biogeochemistry, *Hydrol. Process.*, doi:10.1002/hyp.7196, 2009.
1668 Fröberg, M., Berggren, D., Bergkvist, B., Bryant, C. and Mulder, J.: Concentration and
1669 fluxes of dissolved organic carbon (DOC) in three Norway spruce stands along a climatic
1670 gradient in Sweden, *Biogeochemistry*, doi:10.1007/s10533-004-0564-5, 2006.
1671 Gouttevin, I., Menegoz, M., Dominé, F., Krinner, G., Koven, C., Ciais, P., Tarnocai, C. and
1672 Boike, J.: How the insulating properties of snow affect soil carbon distribution in the

1673 continental pan-Arctic area, *J. Geophys. Res. Biogeosciences*,
1674 doi:10.1029/2011JG001916, 2012.

1675 Graham, D. E., Wallenstein, M. D., Vishnivetskaya, T. A., Waldrop, M. P., Phelps, T. J.,
1676 Pfiffner, S. M., Onstott, T. C., Whyte, L. G., Rivkina, E. M., Gilichinsky, D. A., Elias, D. A.,
1677 MacKelprang, R., Verberkmoes, N. C., Hettich, R. L., Wagner, D., Wulfschleger, S. D. and
1678 Jansson, J. K.: Microbes in thawing permafrost: The unknown variable in the climate
1679 change equation, *ISME J.*, doi:10.1038/ismej.2011.163, 2012.

1680 Guenet, B., Moyano, F. E., Peylin, P., Ciais, P. and Janssens, I. A.: Towards a representation
1681 of priming on soil carbon decomposition in the global land biosphere model ORCHIDEE
1682 (version 1.9.5.2), *Geosci. Model Dev.*, doi:10.5194/gmd-9-841-2016, 2016.

1683 Guenet, B., Camino-Serrano, M., Ciais, P., Tifafi, M., Maignan, F., Soong, J. L. and Janssens,
1684 I. A.: Impact of priming on global soil carbon stocks, *Glob. Chang. Biol.*,
1685 doi:10.1111/gcb.14069, 2018.

1686 Guimberteau, M., Drapeau, G., Ronchail, J., Sultan, B., Polcher, J., Martinez, J. M., Prigent,
1687 C., Guyot, J. L., Cochonneau, G., Espinoza, J. C., Filizola, N., Fraizy, P., Lavado, W., De
1688 Oliveira, E., Pombosa, R., Noriega, L. and Vauchel, P.: Discharge simulation in the sub-
1689 basins of the Amazon using ORCHIDEE forced by new datasets, *Hydrol. Earth Syst. Sci.*,
1690 doi:10.5194/hess-16-911-2012, 2012.

1691 Guimberteau, M., Zhu, D., Maignan, F., Huang, Y., Yue, C., Dantec-N d lec, S., Ottl, C., Jornet-
1692 Puig, A., Bastos, A., Laurent, P., Goll, D., Bowring, S., Chang, J., Guenet, B., Tifafi, M., Peng,
1693 S., Krinner, G., Ducharne, A. s., Wang, F., Wang, T., Wang, X., Wang, Y., Yin, Z., Lauerwald,
1694 R., Joetzjer, E., Qiu, C., Kim, H. and Ciais, P.: ORCHIDEE-MICT (v8.4.1), a land surface
1695 model for the high latitudes: model description and validation, *Geosci. Model Dev.*,
1696 doi:10.5194/gmd-11-121-2018, 2018.

1697 Hastie, A., Lauerwald, R., Weyhenmeyer, G., Sobek, S., Verpoorter, C. and Regnier, P.: CO2
1698 evasion from boreal lakes: Revised estimate, drivers of spatial variability, and future
1699 projections, *Glob. Chang. Biol.*, doi:10.1111/gcb.13902, 2018.

1700 Heim, B., Abramova, E., Doerffer, R., Günther, F., Hölemann, J., Kraberg, A., Lantuit, H.,
1701 Loginova, A., Martynov, F., Overduin, P. P. and Wegner, C.: Ocean colour remote sensing
1702 in the southern laptev sea: Evaluation and applications, *Biogeosciences*, doi:10.5194/bg-
1703 11-4191-2014, 2014.

1704 Hollesen, J., Matthiesen, H., Møller, A. B. and Elberling, B.: Permafrost thawing in organic
1705 Arctic soils accelerated by ground heat production, *Nat. Clim. Chang.*,
1706 doi:10.1038/nclimate2590, 2015.

1707 Holmes, R. M., McClelland, J. W., Peterson, B. J., Tank, S. E., Bulygina, E., Eglinton, T. I.,
1708 Gordeev, V. V., Gurtovaya, T. Y., Raymond, P. A., Repeta, D. J., Staples, R., Striegl, R. G.,
1709 Zhulidov, A. V. and Zimov, S. A.: Seasonal and Annual Fluxes of Nutrients and Organic
1710 Matter from Large Rivers to the Arctic Ocean and Surrounding Seas, *Estuaries and
1711 Coasts*, doi:10.1007/s12237-011-9386-6, 2012.

1712 Hugelius, G., Bockheim, J. G., Camill, P., Elberling, B., Grosse, G., Harden, J. W., Johnson, K.,
1713 Jorgenson, T., Koven, C. D., Kuhry, P., Michaelson, G., Mishra, U., Palmtag, J., Ping, C.-L.,
1714 O'Donnell, J., Schirrmeister, L., Schuur, E. A. G., Sheng, Y., Smith, L. C., Strauss, J. and Yu, Z.:
1715 A new data set for estimating organic carbon storage to 3m depth in soils of the
1716 northern circumpolar permafrost region, *EARTH Syst. Sci. DATA*, doi:10.5194/essd-5-
1717 393-2013, 2013.

1718 Hugelius, G., Strauss, J., Zubrzycki, S., Harden, J. W., Schuur, E. A. G., Ping, C. L.,
1719 Schirrmeister, L., Grosse, G., Michaelson, G. J., Koven, C. D., O'Donnell, J. A., Elberling, B.,
1720 Mishra, U., Camill, P., Yu, Z., Palmtag, J. and Kuhry, P.: Estimated stocks of circumpolar
1721 permafrost carbon with quantified uncertainty ranges and identified data gaps,

1722 Biogeosciences, doi:10.5194/bg-11-6573-2014, 2014.
1723 Jakobsson, M.: Hypsometry and volume of the Arctic Ocean and its constituent seas,
1724 Geochemistry, Geophys. Geosystems, doi:10.1029/2001GC000302, 2002.
1725 Janout, M., Hájek, J., Juhls, B., Krumpen, T., Rabe, B., Bauch, D., Wegner, C., Kassens,
1726 H. and Timokhov, L.: Episodic warming of near-bottom waters under the Arctic sea ice
1727 on the central Laptev Sea shelf, Geophys. Res. Lett., doi:10.1002/2015GL066565, 2016.
1728 Jasechko, S., Kirchner, J. W., Welker, J. M. and McDonnell, J. J.: Substantial proportion of
1729 global streamflow less than three months old, Nat. Geosci., doi:10.1038/ngeo2636, 2016.
1730 Kicklighter, D. W., Hayes, D. J., McClelland, J. W., Peterson, B. J., McGuire, A. D. and Melillo,
1731 J. M.: Insights and issues with simulating terrestrial DOC loading of Arctic river
1732 networks, Ecol. Appl., doi:10.1890/11-1050.1, 2013.
1733 Koven, C., Friedlingstein, P., Ciais, P., Khvorostyanov, D., Krinner, G. and Tarnocai, C.: On
1734 the formation of high-latitude soil carbon stocks: Effects of cryoturbation and insulation
1735 by organic matter in a land surface model, Geophys. Res. Lett.,
1736 doi:10.1029/2009GL040150, 2009.
1737 Koven, C. D., Riley, W. J., Subin, Z. M., Tang, J. Y., Torn, M. S., Collins, W. D., Bonan, G. B.,
1738 Lawrence, D. M. and Swenson, S. C.: The effect of vertically resolved soil biogeochemistry
1739 and alternate soil C and N models on C dynamics of CLM4, Biogeosciences,
1740 doi:10.5194/bg-10-7109-2013, 2013.
1741 Koven, C. D., Schuur, E. A. G., Schädel, C., Bohn, T. J., Burke, E. J., Chen, G., Chen, X., Ciais, P.,
1742 Grosse, G., Harden, J. W., Hayes, D. J., Hugelius, G., Jafarov, E. E., Krinner, G., Kuhry, P.,
1743 Lawrence, D. M., MacDougall, A. H., Marchenko, S. S., McGuire, A. D., Natali, S. M.,
1744 Nicolsky, D. J., Olefeldt, D., Peng, S., Romanovsky, V. E., Schaefer, K. M., Strauss, J., Treat, C.
1745 C. and Turetsky, M.: A simplified, data-constrained approach to estimate the permafrost
1746 carbon-climate feedback, Philos. Trans. R. Soc. A Math. Phys. Eng. Sci.,
1747 doi:10.1098/rsta.2014.0423, 2015.
1748 Krinner, G., Viovy, N., de Noblet-Ducoudré, N., Ogée, J., Polcher, J., Friedlingstein, P., Ciais,
1749 P., Sitch, S. and Prentice, I. C.: A dynamic global vegetation model for studies of the
1750 coupled atmosphere-biosphere system, Global Biogeochem. Cycles,
1751 doi:10.1029/2003GB002199, 2005.
1752 Kunkel, K. E., Robinson, D. A., Champion, S., Yin, X., Estilow, T. and Frankson, R. M.:
1753 Trends and Extremes in Northern Hemisphere Snow Characteristics, Curr. Clim. Chang.
1754 Reports, doi:10.1007/s40641-016-0036-8, 2016.
1755 Kutscher, L., Mörth, C. M., Porcelli, D., Hirst, C., Maximov, T. C., Petrov, R. E. and
1756 Andersson, P. S.: Spatial variation in concentration and sources of organic carbon in the
1757 Lena River, Siberia, J. Geophys. Res. Biogeosciences, doi:10.1002/2017JG003858, 2017.
1758 Lammers, R. B., Pundsack, J. W. and Shiklomanov, A. I.: Variability in river temperature,
1759 discharge, and energy flux from the Russian pan-Arctic landmass, J. Geophys. Res.
1760 Biogeosciences, doi:10.1029/2006JG000370, 2007.
1761 Lauerwald, R., Regnier, P., Camino-Serrano, M., Guenet, B., Guimberteau, M., Ducharne,
1762 A., Polcher, J. and Ciais, P.: ORCHILEAK (revision 3875): A new model branch to simulate
1763 carbon transfers along the terrestrial-aquatic continuum of the Amazon basin, Geosci.
1764 Model Dev., doi:10.5194/gmd-10-3821-2017, 2017.
1765 Lee, H., Swenson, S. C., Slater, A. G. and Lawrence, D. M.: Effects of excess ground ice on
1766 projections of permafrost in a warming climate, Environ. Res. Lett., doi:10.1088/1748-
1767 9326/9/12/124006, 2014.
1768 Lindroos, A. J., Derome, J., Derome, K. and Smolander, A.: The effect of scots pine, norway
1769 spruce and silver birch on the chemical composition of stand throughfall and upper soil
1770 percolation water in northern Finland, Boreal Environ. Res., 2011.

1771 MacKelprang, R., Waldrop, M. P., Deangelis, K. M., David, M. M., Chavarria, K. L.,
1772 Blazewicz, S. J., Rubin, E. M. and Jansson, J. K.: Metagenomic analysis of a permafrost
1773 microbial community reveals a rapid response to thaw, *Nature*,
1774 doi:10.1038/nature10576, 2011.
1775 Mann, P. J., Eglinton, T. I., McIntyre, C. P., Zimov, N., Davydova, A., Vonk, J. E., Holmes, R.
1776 M. and Spencer, R. G. M.: Utilization of ancient permafrost carbon in headwaters of Arctic
1777 fluvial networks, *Nat. Commun.*, doi:10.1038/ncomms8856, 2015.
1778 Manning, R.: On the Flow of Water in Open Channels and Pipes, *Trans. Inst. Civ. Eng. Irel.*,
1779 doi:10.1021/bi2010619, 1891.
1780 Manzoni, S., Taylor, P., Richter, A., Porporato, A. and Ågren, G. I.: Environmental and
1781 stoichiometric controls on microbial carbon-use efficiency in soils, *New Phytol.*,
1782 doi:10.1111/j.1469-8137.2012.04225.x, 2012.
1783 McClelland, J. W., Holmes, R. M., Dunton, K. H. and Macdonald, R. W.: The Arctic Ocean
1784 Estuary, *Estuaries and Coasts*, doi:10.1007/s12237-010-9357-3, 2012.
1785 McClelland, J. W., Holmes, R. M., Peterson, B. J., Raymond, P. A., Striegl, R. G., Zhulidov, A.
1786 V., Zimov, S. A., Zimov, N., Tank, S. E., Spencer, R. G. M., Staples, R., Gurtovaya, T. Y. and
1787 Griffin, C. G.: Particulate organic carbon and nitrogen export from major Arctic rivers,
1788 *Global Biogeochem. Cycles*, doi:10.1002/2015GB005351, 2016.
1789 McGuire, A. D., Anderson, L. G., Christensen, T. R., Dallimore, S., Guo, L., Hayes, D. J.,
1790 Heimann, M., Lorenson, T. D., Macdonald, R. W. and Roulet, N.: Sensitivity of the carbon
1791 cycle in the Arctic to climate change, *Ecol. Monogr.*, doi:10.1890/08-2025.1, 2009.
1792 Messenger, M. L., Lehner, B., Grill, G., Nedeva, I. and Schmitt, O.: Estimating the volume and
1793 age of water stored in global lakes using a geo-statistical approach, *Nat. Commun.*,
1794 doi:10.1038/ncomms13603, 2016.
1795 Mudryk, L. R., Derksen, C., Kushner, P. J. and Brown, R.: Characterization of Northern
1796 Hemisphere snow water equivalent datasets, 1981-2010, *J. Clim.*, doi:10.1175/JCLI-D-
1797 15-0229.1, 2015.
1798 Myers-Pigg, A. N., Louchouart, P., Amon, R. M. W., Prokushkin, A., Pierce, K. and Rubtsov,
1799 A.: Labile pyrogenic dissolved organic carbon in major Siberian Arctic rivers:
1800 Implications for wildfire-stream metabolic linkages, *Geophys. Res. Lett.*,
1801 doi:10.1002/2014GL062762, 2015.
1802 Nachtergaele, F. et al.: The harmonized world soil database, FAO, ISRIC, ISSCAS, JRC,
1803 doi:3123, 2010.
1804 Ngo-Duc, T., Laval, K., Ramillien, G., Polcher, J. and Cazenave, A.: Validation of the land
1805 water storage simulated by Organising Carbon and Hydrology in Dynamic Ecosystems
1806 (ORCHIDEE) with Gravity Recovery and Climate Experiment (GRACE) data, *Water*
1807 *Resour. Res.*, doi:10.1029/2006WR004941, 2007.
1808 O'Donnell, J. A., Aiken, G. R., Swanson, D. K., Panda, S., Butler, K. D. and Baltensperger, A.
1809 P.: Dissolved organic matter composition of Arctic rivers: Linking permafrost and parent
1810 material to riverine carbon, *Global Biogeochem. Cycles*, doi:10.1002/2016GB005482,
1811 2016.
1812 Oki, T., Nishimura, T. and Dirmeyer, P. A.: Assessment of annual runoff from land surface
1813 models using Total Runoff Integrating Pathways (TRIP), *J. Meteorol. Soc. Japan*, 1999.
1814 Parton, W. J., Schimel, D. S., Cole, C. V. and Ojima, D. S.: Analysis of Factors Controlling
1815 Soil Organic Matter Levels in Great Plains Grasslands, *Soil Sci. Soc. Am. J.*, 1987.
1816 Pekel, J.-F., Cottam, A., Gorelick, N. and Belward, A. S.: Global Surface Water - Data Users
1817 Guide (JRC) High-resolution mapping of global surface water and its long-term changes,
1818 *Nature*, doi:10.1038/nature20584, 2016.
1819 Peterson, B. J., Holmes, R. M., McClelland, J. W., Vörösmarty, C. J., Lammers, R. B.,

1820 Shiklomanov, A. I., Shiklomanov, I. A. and Rahmstorf, S.: Increasing river discharge to the
1821 Arctic Ocean, *Science* (80-.), doi:10.1126/science.1077445, 2002.
1822 Ponomarev, E. I., Kharuk, V. I. and Ranson, K. J.: Wildfires dynamics in Siberian larch
1823 forests, *Forests*, doi:10.3390/f7060125, 2016.
1824 Prigent, C., Papa, F., Aires, F., Rossow, W. B. and Matthews, E.: Global inundation
1825 dynamics inferred from multiple satellite observations, 1993-2000, *J. Geophys. Res.*
1826 *Atmos.*, doi:10.1029/2006JD007847, 2007.
1827 Qiu, C., Zhu, D., Ciais, P., Guenet, B., Krinner, G., Peng, S., Aurela, M., Bernhofer, C.,
1828 Brümmer, C., Bret-Harte, S., Chu, H., Chen, J., Desai, A. R., Dušek, J., Euskirchen, E. S.,
1829 Fortuniak, K., Flanagan, L. B., Friborg, T., Grygoruk, M., Gogo, S., Grünwald, T., Hansen, B.
1830 U., Holl, D., Humphreys, E., Hurkuck, M., Kiely, G., Klatt, J., Kutzbach, L., Langeron, C.,
1831 Laggoun-Défarage, F., Lund, M., Lafleur, P. M., Li, X., Mammarella, I., Merbold, L., Nilsson,
1832 M. B., Olejnik, J., Ottosson-Löfvenius, M., Oechel, W., Parmentier, F. J. W., Peichl, M., Pirk,
1833 N., Peltola, O., Pawlak, W., Rasse, D., Rinne, J., Shaver, G., Peter Schmid, H., Sottocornola,
1834 M., Steinbrecher, R., Sachs, T., Urbaniak, M., Zona, D. and Ziemblinska, K.: ORCHIDEE-
1835 PEAT (revision 4596), a model for northern peatland CO₂, water, and energy fluxes on
1836 daily to annual scales, *Geosci. Model Dev.*, doi:10.5194/gmd-11-497-2018, 2018.
1837 Raymond, P. A., McClelland, J. W., Holmes, R. M., Zhulidov, A. V., Mull, K., Peterson, B. J.,
1838 Striegl, R. G., Aiken, G. R. and Gurtovaya, T. Y.: Flux and age of dissolved organic carbon
1839 exported to the Arctic Ocean: A carbon isotopic study of the five largest arctic rivers,
1840 *Global Biogeochem. Cycles*, doi:10.1029/2007GB002934, 2007.
1841 Rhein, M., Rintoul, S., Aoki, S., Campos, E., Chambers, D., Feely, R. A., Gulev, S., Johnson, G.,
1842 Josey, S., Kostianoy, A., Mauritzen, C., Roemmich, D., Talley, L., Wang, F. and IPCC:
1843 Observations: Ocean. In: *Climate Change 2013: The Physical Science Basis. Contribution*
1844 *of Working Group I to the Fifth Assessment Report of the Intergovernmental Panel on*
1845 *Climate Change.*, 2013.
1846 Rosenqvist, L., Hansen, K., Vesterdal, L. and van der Salm, C.: Water balance in
1847 afforestation chronosequences of common oak and Norway spruce on former arable
1848 land in Denmark and southern Sweden, *Agric. For. Meteorol.*,
1849 doi:10.1016/j.agrformet.2009.10.004, 2010.
1850 Schuur, E. A. G., Vogel, J. G., Crummer, K. G., Lee, H., Sickman, J. O. and Osterkamp, T. E.:
1851 The effect of permafrost thaw on old carbon release and net carbon exchange from
1852 tundra, *Nature*, doi:10.1038/nature08031, 2009.
1853 Schuur, E. A. G., McGuire, A. D., Schädel, C., Grosse, G., Harden, J. W., Hayes, D. J., Hugelius,
1854 G., Koven, C. D., Kuhry, P., Lawrence, D. M., Natali, S. M., Olefeldt, D., Romanovsky, V. E.,
1855 Schaefer, K., Turetsky, M. R., Treat, C. C. and Vonk, J. E.: Climate change and the
1856 permafrost carbon feedback, *Nature*, doi:10.1038/nature14338, 2015.
1857 Selvam, B. P., Lapierre, J. F., Guillemette, F., Voigt, C., Lamprecht, R. E., Biasi, C.,
1858 Christensen, T. R., Martikainen, P. J. and Berggren, M.: Degradation potentials of
1859 dissolved organic carbon (DOC) from thawed permafrost peat, *Sci. Rep.*,
1860 doi:10.1038/srep45811, 2017.
1861 Serreze, M. C. and Barry, R. G.: Processes and impacts of Arctic amplification: A research
1862 synthesis, *Glob. Planet. Change*, doi:10.1016/j.gloplacha.2011.03.004, 2011.
1863 Shakhova, N., Semiletov, I., Sergienko, V., Lobkovsky, L., Yusupov, V., Salyuk, A.,
1864 Salomatin, A., Chernykh, D., Kosmach, D., Panteleev, G., Nicolsky, D., Samarkin, V., Joye, S.,
1865 Charkin, A., Dudarev, O., Meluzov, A. and Gustafsson, O.: The East Siberian Arctic Shelf:
1866 Towards further assessment of permafrost-related methane fluxes and role of sea ice,
1867 *Philos. Trans. R. Soc. A Math. Phys. Eng. Sci.*, doi:10.1098/rsta.2014.0451, 2015.
1868 Smith, L. C. and Pavelsky, T. M.: Estimation of river discharge, propagation speed, and

1869 hydraulic geometry from space: Lena River, Siberia, *Water Resour. Res.*,
1870 doi:10.1029/2007WR006133, 2008.
1871 Sorokin, Y. I. and Sorokin, P. Y.: Plankton and primary production in the Lena River
1872 Estuary and in the south-eastern Laptev sea, *Estuar. Coast. Shelf Sci.*,
1873 doi:10.1006/ecss.1996.0078, 1996.
1874 Spencer, R. G. M., Mann, P. J., Dittmar, T., Eglinton, T. I., McIntyre, C., Holmes, R. M., Zimov,
1875 N. and Stubbins, A.: Detecting the signature of permafrost thaw in Arctic rivers, *Geophys.*
1876 *Res. Lett.*, doi:10.1002/2015GL063498, 2015.
1877 Starr, M., Lindroos, A. J., Ukonmaanaho, L., Tarvainen, T. and Tanskanen, H.: Weathering
1878 release of heavy metals from soil in comparison to deposition, litterfall and leaching
1879 fluxes in a remote, boreal coniferous forest, *Appl. Geochemistry*, doi:10.1016/S0883-
1880 2927(02)00157-9, 2003.
1881 Steele, M. and Ermold, W.: Loitering of the retreating sea ice edge in the Arctic Seas, *J.*
1882 *Geophys. Res. Ocean.*, doi:10.1002/2015JC011182, 2015.
1883 Stroeve, J. C., Markus, T., Boisvert, L., Miller, J. and Barrett, A.: Changes in Arctic melt
1884 season and implications for sea ice loss, *Geophys. Res. Lett.*,
1885 doi:10.1002/2013GL058951, 2014.
1886 Stubbins, A., Mann, P. J., Powers, L., Bittar, T. B., Dittmar, T., McIntyre, C. P., Eglinton, T. I.,
1887 Zimov, N. and Spencer, R. G. M.: Low photolability of yedoma permafrost dissolved
1888 organic carbon, *J. Geophys. Res. Biogeosciences*, doi:10.1002/2016JG003688, 2017.
1889 Suzuki, K., Konohira, E., Yamazaki, Y., Kubota, J., Ohata, T. and Vuglinsky, V.: Transport of
1890 organic carbon from the Mogot Experimental Watershed in the southern mountainous
1891 taiga of eastern Siberia, *Hydrol. Res.*, doi:10.2166/nh.2006.015, 2006.
1892 Suzuki, K., Matsuo, K., Yamazaki, D., Ichii, K., Iijima, Y., Papa, F., Yanagi, Y. and Hiyama, T.:
1893 Hydrological variability and changes in the Arctic circumpolar tundra and the three
1894 largest pan-Arctic river basins from 2002 to 2016, *Remote Sens.*,
1895 doi:10.3390/rs10030402, 2018.
1896 Tank, S. E., Fellman, J. B., Hood, E. and Kritzberg, E. S.: Beyond respiration: Controls on
1897 lateral carbon fluxes across the terrestrial-aquatic interface, *Limnol. Oceanogr. Lett.*,
1898 doi:10.1002/lol2.10065, 2018.
1899 Tarnocai, C., Canadell, J. G., Schuur, E. A. G., Kuhry, P., Mazhitova, G. and Zimov, S.: Soil
1900 organic carbon pools in the northern circumpolar permafrost region, *Global Biogeochem.*
1901 *Cycles*, doi:10.1029/2008gb003327, 2009.
1902 Tootchi, A., Jost, A. and Ducharme, A.: Multi-source global wetland maps combining
1903 surface water imagery and groundwater constraints, *Earth Syst. Sci. Data*,
1904 doi:10.5194/essd-11-189-2019, 2019.
1905 Venkiteswaran, J. J., Schiff, S. L. and Wallin, M. B.: Large carbon dioxide fluxes from
1906 headwater boreal and sub-boreal streams, *PLoS One*,
1907 doi:10.1371/journal.pone.0101756, 2014.
1908 Vitousek, P. M. and Hobbie, S.: Heterotrophic nitrogen fixation in decomposing litter:
1909 Patterns and regulation, *Ecology*, doi:10.1890/0012-
1910 9658(2000)081[2366:HNFIDL]2.0.CO;2, 2000.
1911 Vitousek, P. M. and Sanford, R. L.: Nutrient Cycling in Moist Tropical Forest, *Ecology*,
1912 doi:10.1146/annurev.es.17.110186.001033, 1986.
1913 Van Vliet, M. T. H., Yearsley, J. R., Franssen, W. H. P., Ludwig, F., Haddeland, I.,
1914 Lettenmaier, D. P. and Kabat, P.: Coupled daily streamflow and water temperature
1915 modelling in large river basins, *Hydrol. Earth Syst. Sci.*, doi:10.5194/hess-16-4303-2012,
1916 2012.
1917 Van Vliet, M. T. H., Franssen, W. H. P., Yearsley, J. R., Ludwig, F., Haddeland, I.,

1918 Lettenmaier, D. P. and Kabat, P.: Global river discharge and water temperature under
1919 climate change, *Glob. Environ. Chang.*, doi:10.1016/j.gloenvcha.2012.11.002, 2013.
1920 Vonk, J. E., Mann, P. J., Davydov, S., Davydova, A., Spencer, R. G. M., Schade, J., Sobczak, W.
1921 V., Zimov, N., Zimov, S., Bulygina, E., Eglinton, T. I. and Holmes, R. M.: High biolability of
1922 ancient permafrost carbon upon thaw, *Geophys. Res. Lett.*, doi:10.1002/grl.50348, 2013.
1923 Vonk, J. E., Tank, S. E., Mann, P. J., Spencer, R. G. M., Treat, C. C., Striegl, R. G., Abbott, B. W.
1924 and Wickland, K. P.: Biodegradability of dissolved organic carbon in permafrost soils and
1925 aquatic systems: A meta-analysis, *Biogeosciences*, doi:10.5194/bg-12-6915-2015,
1926 2015a.
1927 Vonk, J. E., Tank, S. E., Bowden, W. B., Laurion, I., Vincent, W. F., Alekseychik, P., Amyot,
1928 M., Billet, M. F., Canário, J., Cory, R. M., Deshpande, B. N., Helbig, M., Jammet, M., Karlsson,
1929 J., Larouche, J., MacMillan, G., Rautio, M., Walter Anthony, K. M. and Wickland, K. P.:
1930 Reviews and Syntheses: Effects of permafrost thaw on arctic aquatic ecosystems,
1931 *Biogeosciences Discuss.*, doi:10.5194/bgd-12-10719-2015, 2015b.
1932 Vorosmarty, C. J., Fekete, B. M., Meybeck, M. and Lammers, R. B.: Global system of rivers:
1933 Its role in organizing continental land mass and defining land-To-Ocean linkages, *Global*
1934 *Biogeochem. Cycles*, doi:10.1029/1999GB900092, 2000.
1935 Walz, J., Knoblauch, C., Böhme, L. and Pfeiffer, E. M.: Regulation of soil organic matter
1936 decomposition in permafrost-affected Siberian tundra soils - Impact of oxygen
1937 availability, freezing and thawing, temperature, and labile organic matter, *Soil Biol.*
1938 *Biochem.*, doi:10.1016/j.soilbio.2017.03.001, 2017.
1939 Wang, T., Ottlé, C., Boone, A., Ciais, P., Brun, E., Morin, S., Krinner, G., Piao, S. and Peng, S.:
1940 Evaluation of an improved intermediate complexity snow scheme in the ORCHIDEE land
1941 surface model, *J. Geophys. Res. Atmos.*, doi:10.1002/jgrd.50395, 2013.
1942 Wanninkhof, R.: Relationship between wind speed and gas exchange over the ocean
1943 revisited, *Limnol. Oceanogr. Methods*, doi:10.4319/lom.2014.12.351, 2014.
1944 Wanninkhof, R. H.: Relationship between wind speed and gas exchange, *J. Geophys. Res.*,
1945 doi:10.1029/92JC00188, 1992.
1946 Whitefield, J., Winsor, P., McClelland, J. and Menemenlis, D.: A new river discharge and
1947 river temperature climatology data set for the pan-Arctic region, *Ocean Model.*,
1948 doi:10.1016/j.ocemod.2014.12.012, 2015.
1949 Wickland, K. P., Waldrop, M. P., Aiken, G. R., Koch, J. C., Jorgenson, M. T. and Striegl, R. G.:
1950 Dissolved organic carbon and nitrogen release from boreal Holocene permafrost and
1951 seasonally frozen soils of Alaska, *Environ. Res. Lett.*, doi:10.1088/1748-9326/aac4ad,
1952 2018.
1953 Wild, B., Schneckner, J., Alves, R. J. E., Barsukov, P., Bárta, J., Čapek, P., Gentsch, N., Gittel, A.,
1954 Guggenberger, G., Lashchinskiy, N., Mikutta, R., Rusalimova, O., Šantrůčková, H.,
1955 Shibistova, O., Urich, T., Watzka, M., Zrazhevskaya, G. and Richter, A.: Input of easily
1956 available organic C and N stimulates microbial decomposition of soil organic matter in
1957 arctic permafrost soil, *Soil Biol. Biochem.*, doi:10.1016/j.soilbio.2014.04.014, 2014.
1958 Wild, B., Gentsch, N., Čapek, P., Diáková, K., Alves, R. J. E., Bárta, J., Gittel, A., Hugelius, G.,
1959 Knoltsch, A., Kuhry, P., Lashchinskiy, N., Mikutta, R., Palmtag, J., Schleper, C., Schneckner, J.,
1960 Shibistova, O., Takriti, M., Torsvik, V. L., Urich, T., Watzka, M., Šantrůčková, H.,
1961 Guggenberger, G. and Richter, A.: Plant-derived compounds stimulate the decomposition
1962 of organic matter in arctic permafrost soils, *Sci. Rep.*, doi:10.1038/srep25607, 2016.
1963 Woods, G. C., Simpson, M. J., Pautler, B. G., Lamoureux, S. F., Lafrenière, M. J. and Simpson,
1964 A. J.: Evidence for the enhanced lability of dissolved organic matter following permafrost
1965 slope disturbance in the Canadian High Arctic, *Geochim. Cosmochim. Acta*,
1966 doi:10.1016/j.gca.2011.08.013, 2011.

1967 Wu, Y., Clarke, N. and Mulder, J.: Dissolved organic carbon concentrations in throughfall
 1968 and soil waters at level II monitoring plots in norway: Short- and long-term variations,
 1969 Water. Air. Soil Pollut., doi:10.1007/s11270-009-0073-1, 2010.
 1970 Xue, K.: Tundra soil carbon is vulnerable to rapid microbial decomposition under
 1971 climatewarming, Nat. Clim. Chang, doi:10.1038/NCLIMATE2940, 2017.
 1972 Ye, B., Yang, D., Zhang, Z. and Kane, D. L.: Variation of hydrological regime with
 1973 permafrost coverage over Lena Basin in Siberia, J. Geophys. Res. Atmos.,
 1974 doi:10.1029/2008JD010537, 2009.
 1975 Yu, Z.: Holocene carbon flux histories of the world's peatlands: Global carbon-cycle
 1976 implications, Holocene, doi:10.1177/0959683610386982, 2011.
 1977 Yue, C., Ciais, P., Zhu, D., Wang, T., Peng, S. S. and Piao, S. L.: How have past fire
 1978 disturbances contributed to the current carbon balance of boreal ecosystems?,
 1979 Biogeosciences, doi:10.5194/bg-13-675-2016, 2016.
 1980 Zhang, K., Kimball, J. S., Mu, Q., Jones, L. A., Goetz, S. J. and Running, S. W.: Satellite based
 1981 analysis of northern ET trends and associated changes in the regional water balance
 1982 from 1983 to 2005, J. Hydrol., doi:10.1016/j.jhydrol.2009.09.047, 2009.
 1983 Zhang, X., Hutchings, J. A., Bianchi, T. S., Liu, Y., Arellano, A. R. and Schuur, E. A. G.:
 1984 Importance of lateral flux and its percolation depth on organic carbon export in Arctic
 1985 tundra soil: Implications from a soil leaching experiment, J. Geophys. Res.
 1986 Biogeosciences, doi:10.1002/2016JG003754, 2017.
 1987 Zhu, D., Peng, S., Ciais, P., Zech, R., Krinner, G., Zimov, S. and Grosse, G.: Simulating soil
 1988 organic carbon in yedoma deposits during the Last Glacial Maximum in a land surface
 1989 model, Geophys. Res. Lett., doi:10.1002/2016GL068874, 2016.
 1990 Zubrzycki, S., Kutzbach, L., Grosse, G. and Desyatkin, A.: Organic carbon and total
 1991 nitrogen stocks in soils of the Lena River Delta, Biogeosciences, doi:10.5194/bg-10-
 1992 3507-2013, 2013.

Tables and Figures:

Table 1: Data type, name and sources of data files used to drive the model in the study simulations.

Data Type	Name	Source
Vegetation Map	ESA CCI Land Cover Map	Bontemps et al., 2013
Topographic Index	STN-30p	Vörösmarty et al., 2000
Stream flow direction	STN-30p	Vörösmarty et al., 2000
River surface area		Lauerwald et al., 2015
Soil texture class		Reynolds et al. 1999
Climatology	GSWP3 v0, 1 degree	http://hydro.iis.u-tokyo.ac.jp/GSWP3/
Potential floodplains	Multi-source global wetland maps	Tootchi et al., 2019
Poor soils	Harmonized World Soil Database map	Nachtergaele et al., 2010
Spinup Soil Carbon Stock	20ky ORCHIDEE-MICT soil carbon spinup	Based on config. in Guimberteau et al. (2018)

1999
 2000
 2001
 2002

Mis en forme: Vérifier l'orthographe et la grammaire

Simon Bowring 31/5/y 12:21

Mis en forme: Anglais (G.B.), Vérifier l'orthographe et la grammaire

Simon Bowring 31/5/y 12:21

Mis en forme: Anglais (G.B.), Vérifier l'orthographe et la grammaire

Simon Bowring 31/5/y 12:21

Mis en forme: Anglais (G.B.), Vérifier l'orthographe et la grammaire

Simon Bowring 31/5/y 12:21

Mis en forme: Anglais (G.B.), Vérifier l'orthographe et la grammaire

Simon Bowring 31/5/y 12:21

Mis en forme: Anglais (G.B.), Vérifier l'orthographe et la grammaire

Simon Bowring 31/5/y 12:21

Mis en forme: Anglais (G.B.), Vérifier l'orthographe et la grammaire

Simon Bowring 31/5/y 12:21

Mis en forme: Anglais (G.B.), Vérifier l'orthographe et la grammaire

Simon Bowring 31/5/y 12:21

Mis en forme ... [124]

Simon Bowring 31/5/y 12:21

Mis en forme: Anglais (G.B.), Vérifier l'orthographe et la grammaire

Simon Bowring 30/5/y 14:42

Supprimé: 9

Simon Bowring 31/5/y 12:21

Mis en forme: Anglais (G.B.), Vérifier l'orthographe et la grammaire

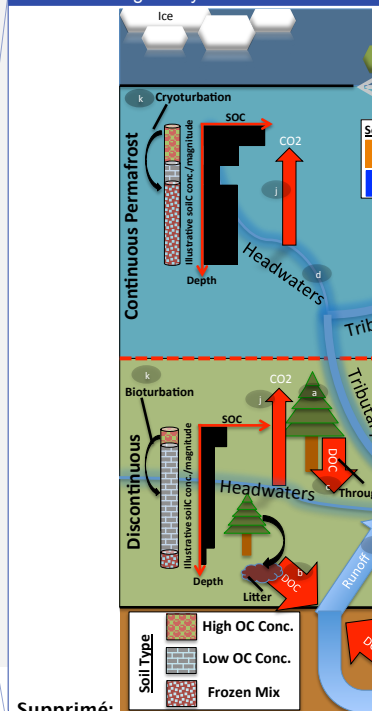
Simon Bowring 31/5/y 12:21

Mis en forme: Anglais (G.B.), Vérifier l'orthographe et la grammaire

Simon Bowring 31/5/y 12:21

Mis en forme: Vérifier l'orthographe et la grammaire

Simon Bowring 30/5/y 17:07



Supprimé:

Simon Bowring 31/5/y 12:21

Mis en forme: Vérifier l'orthographe et la grammaire

2007
2008
2009
2010
2011
2012
2013
2014
2015
2016
2017
2018
2019
2020
2021
2022
2023
2024
2025
2026
2027
2028
2029
2030
2031
2032

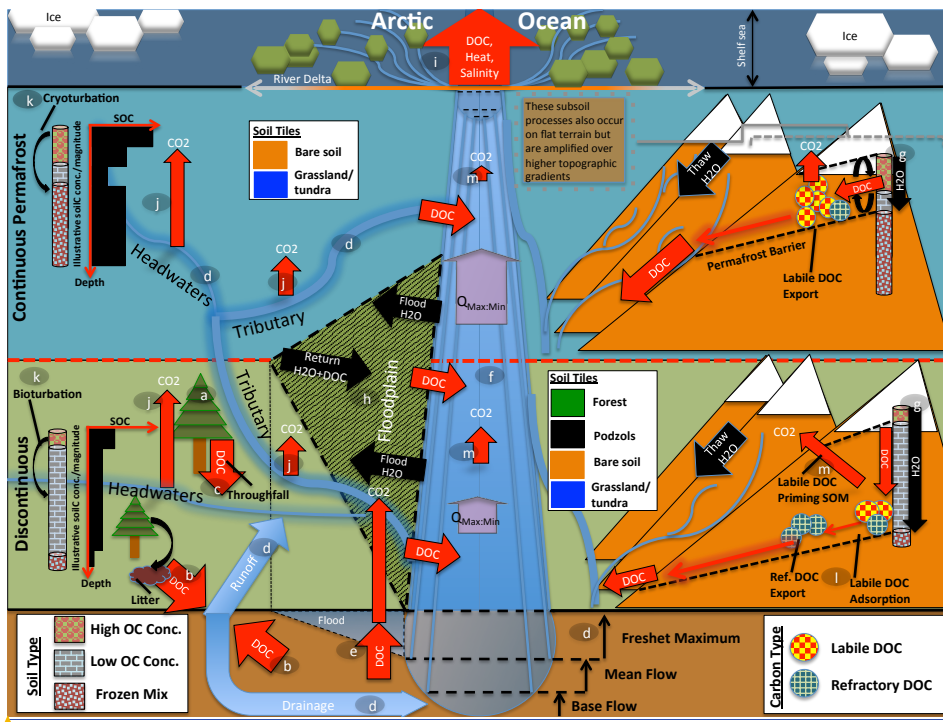
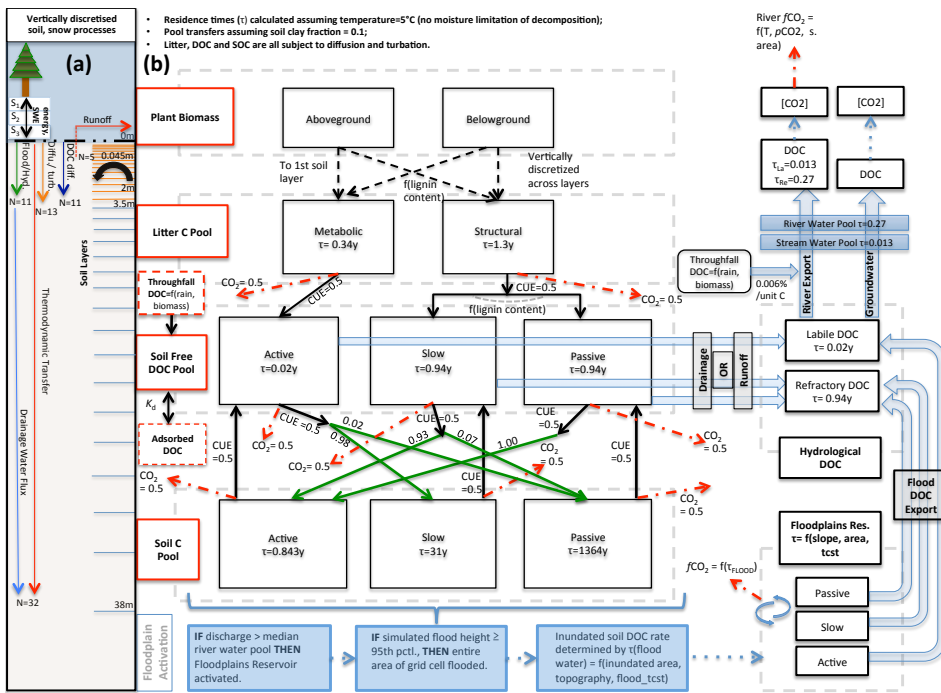


Figure 1: Cartoon diagram illustrating the landscape-scale emergent phenomena observed in high-latitude river systems that are captured by the processes represented in this model. Here, the terrestrial area is shown, in vertically-ascending order, as subsoil, discontinuous permafrost, continuous permafrost and the maritime boundary. Note that 'tributaries' in the Figure may be represented in the model by either the 'fast' or 'stream' pool, depending on their size. Representative soil types, their distributions and carbon concentrations are shown for the two permafrost zones, as well as the different dynamics occurring on 'flat' (left) and 'sloping' land (right) arising from their permafrost designation. Carbon exports from one subsystem to another are shown in red. The relative strength of the same processes occurring in each permafrost band are indicated by relative arrow size. Note that the high CO₂ evasion in headwaters versus tributaries versus mainstem is shown here. Proposed and modelled mechanisms of soil carbon priming, adsorption and rapid metabolisation are shown. The arrows $Q_{Max:Min}$ refer to the ratio of maximum to minimum discharge at a given point in the river, the ratio indicating hydrologic volatility, whose magnitude is influenced by permafrost coverage. Soil tiles, a model construct used for modulating soil permeability and implicit/explicit decomposition, are shown to indicate the potential differences in these dynamics for the relevant permafrost zones. Note that the marine shelf sea system, as shown in the uppermost rectangle, is not simulated in this model, although our outputs can be coupled for that purpose. Letter markings mark processes of carbon flux in permafrost regions and implicitly or explicitly included in the model, and can be referred to in subsections of the Methods text. These refer to: (a) Biomass generation; (b) DOC generation and leaching; (c) Throughfall and its DOC; (d) Hydrological mobilisation of soil DOC; (e) Soil flooding; (f) Landscape routing of water and carbon; (g)

Unknown
Mis en forme: Police :Gras
Simon Bowring 31/5/y 12:21
Mis en forme: Vérifier l'orthographe et la grammaire

Simon Bowring 31/5/y 12:21
Mis en forme: Vérifier l'orthographe et la grammaire

2033 Infiltration and topography; (h) Floodplain representation; (i) Oceanic outflow; (j)
 2034 Dissolved carbon export and riverine atmospheric evasion; (k) Turbation and soil
 2035 carbon with depth (e.g. (Hugelius et al., 2013; Tarnocai et al., 2009), (Koven et al.,
 2036 2015)); (l) Adsorption; (m) Priming.



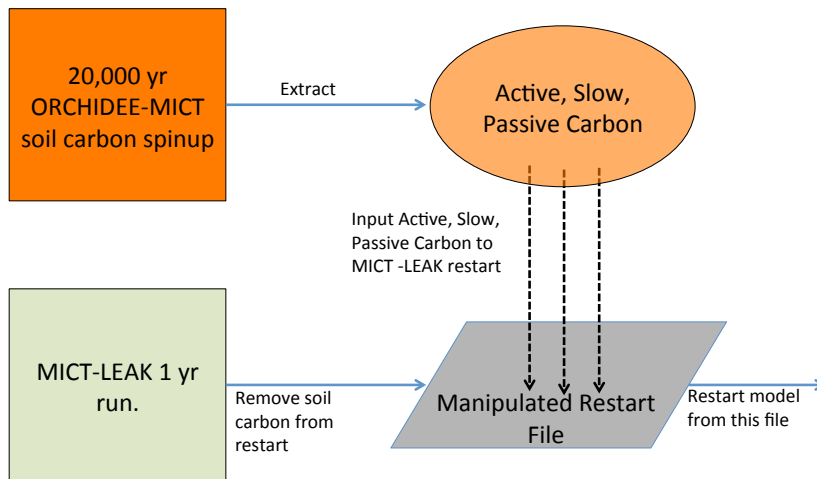
2039
 2040
 2041
 2042 **Figure 2** :Carbon and water flux map for core DOC elements in model structure relating
 2043 to DOC transport and transformation. **(a)** Summary of the differing extent of vertical
 2044 discretisation of soil and snow for different processes calculated in the model.
 2045 Discretisation occurs along 32 layers whose thickness increases geometrically from 0-
 2046 38m. N refers to the number of layers, SWE=snow water equivalent, S_n = Snow layer n.
 2047 Orange layers indicate the depth to which diffusive carbon (turbation) fluxes occur. **(b)**
 2048 Conceptual map of the production, transfer and transformation of carbon in its vertical
 2049 and lateral (i.e., hydrological) flux as calculated in the model. Red boxes indicate meta-
 2050 reservoirs of carbon, black boxes the actual pools as they exist in the model. Black
 2051 arrows indicate carbon fluxes between pools, dashed red arrows give carbon loss as CO₂,
 2052 green arrows highlight the fractional distribution of DOC to SOC (no carbon loss
 2053 incurred in this transfer), a feature of this model. For a given temperature (5°C) and soil
 2054 clay fraction, the fractional fluxes between pools are given for each flux, while residence
 2055 times for each pool (τ) are in each box. The association of carbon dynamics with the
 2056 hydrological module are shown by the blue arrows. Blue coloured boxes illustrate the
 2057 statistical sequence which activates the boolean floodplains module. Note that for

Simon Bowring 31/5/y 12:21
 Mis en forme: Vérifier l'orthographe et la grammaire

Simon Bowring 31/5/y 12:21
 Mis en forme: Vérifier l'orthographe et la grammaire

Simon Bowring 30/5/y 16:48
 Supprimé: dashed

2059 readability, the generation and lateral flux of dissolved CO₂ is omitted from this diagram,
2060 but is described at length in the Methods section.
2061



2062 **Figure 3:** Flow diagram illustrating the step-wise stages required to implement the
2063 model's soil carbon stock prior to conducting transient, historical simulations.
2064

Simon Bowring 31/5/y 12:21
Mis en forme: Vérifier l'orthographe et la grammaire